

WATER QUALITY MODEL  
OF  
YORK RIVER, VIRGINIA

by  
Paul V. Hyer

A Report to the Hampton Roads  
Water Quality Agency

Special Report No. 146  
in Applied Marine Science and  
Ocean Engineering

Virginia Institute of Marine Science  
Gloucester Point, Virginia 23062

William J. Hargis, Jr.  
Director

November, 1977

WATER QUALITY MODEL  
of  
YORK RIVER, VIRGINIA

by

Paul V. Hyer

A Report to the Hampton Roads Water Quality Agency

Special Report No. 146  
in Applied Marine Science and  
Ocean Engineering

The preparation of this report was financed through  
a grant from the U. S. Environmental Protection Agency  
under Section 208 of the Federal Water Pollution Control  
Act Amendments of 1972.

Virginia Institute of Marine Science  
Gloucester Point, Virginia

William J. Hargis, Jr.  
Director

November, 1977

## TABLE OF CONTENTS

	<u>Page</u>
List of Figures . . . . .	iii
List of Tables. . . . .	iv
Acknowledgements. . . . .	v
Abstract. . . . .	1
I. Introduction. . . . .	1
II. Description of Study Area . . . . .	3
III. Description of the Water Quality Model. . . . .	8
A. Biochemical Interactions. . . . .	8
B. Hydraulic Processes . . . . .	8
1. Longitudinal. . . . .	8
2. Vertical. . . . .	13
3. Lateral . . . . .	13
C. Method of Solution. . . . .	13
D. Evaluation of Parameters and Rate Constants . . . . .	18
1. Hydraulic Inputs. . . . .	18
2. Biochemical Inputs. . . . .	20
IV. Model Calibration and Verification. . . . .	28
A. Calibration Procedure . . . . .	28
B. Model Sensitivity . . . . .	40
C. Discussion. . . . .	61
V. Summary and Conclusions . . . . .	65
References. . . . .	66
Appendix A. Input Constants. . . . .	70

## LIST OF FIGURES

	<u>Page</u>
1. Downstream sub-basin of York drainage basin . . . . .	4
2. York and Pamunkey time of slack water relative to York River mouth. . . . .	6
3. York River calculated tidal prism . . . . .	7
4. Schematic Diagram of Interaction of Ecosystem Model	9
5. The York River showing model segments and benthic oxygen demand sampling sites. . . . .	24
6-15. Comparison of calibration results with field observations for salinity, organic nitrogen, ammonia nitrogen, nitrite-nitrate nitrogen, organic phosphorus, inorganic phosphorus, chlorophyll, CBOD, dissolved oxygen and fecal coliform . . . . .	29-38
16-24. Comparison of verification predictions with field observations for salinity, organic nitrogen, ammonia nitrogen, nitrate-nitrite nitrogen, organic phosphorus, inorganic phosphorus, chlorophyll, UBOD, and dissolved oxygen. . . . .	41-49
25. Model predictions for CBOD with point source loads altered . . . . .	51
26-33. Sensitivity of model predictions to variations in input parameters. . . . .	53-60

LIST OF TABLES

	<u>Page</u>
1. Flow records for Beulahville and Hanover, Virginia, 1976 . . . . .	19
2. Benthic oxygen demand studies, York River, 1976. . .	23
3. Point sources of loading used in calibration and verification . . . . .	39

## ACKNOWLEDGEMENTS

This study was carried out with support from the U. S. Environmental Protection Agency through the Hampton Roads Water Quality Agency under section 208 of the Federal Water Pollution Control Act Amendments of 1972.

The development of a portion of the model was funded by the Virginia State Water Control Board, through the Cooperative State Agencies Program with VIMS. In particular, the formulation of the basic equations describing the biochemical interactions was supported by this program.

The intensive field survey, slack water surveys and the applications of the model were funded through the Hampton Roads 208 Study. Nonpoint source loading data was provided by Malcolm Pirnie Engineers, Inc., through the Hampton Roads Water Quality Agency.

We thank Ms. Cathy Garrett for her patient typing of this report and our many colleagues for their helpful comments.

## ABSTRACT

A ten-component time-dependent Phytoplankton Ecosystem model was calibrated and verified for the York Estuary. Since the York is both wide and deep and is characterized by low dissolved oxygen levels in the deeper layer, this model has two layers and three compartments laterally per layer. The calibrated and verified model is suitable for use in studying water quality in the York, such as the development of waste load allocations.

## I. INTRODUCTION

Previous work (Hyer, et al., 1975) in the York River concerned a time-dependent water quality model having four components, namely, salinity, dissolved oxygen, carbonaceous BOD and nitrogenous BOD. This model was one-dimensional, i.e., averaged over cross-section. However, the York River is deeper than ten meters for most of its length and in places approaches thirty meters. Thus, in the summer when water temperatures exceed 20°C, dissolved oxygen stratification occurs even though tidal current amplitude is greater than 1 ft/sec (0.3 m/sec). Data reported by Jordan (1975) show the normally occurring summertime dissolved oxygen difference

between surface and twenty meters to be five mg/l to seven mg/l or greater. Hence, the deeper waters frequently fell below three mg/l of dissolved oxygen. This dissolved oxygen stratification has been observed with varying degrees of salinity stratification from two parts per thousand to six parts per thousand.

In view of this dissolved oxygen stratification, a two-layer model was required for the York River. Furthermore, the width of this estuary (up to two nautical miles or 3.7 km) indicated the use of lateral segmentation. The model to be used has three lateral compartments in each of two layers, or six compartments per longitudinal reach. Hence, it is called a quasi-three-dimensional model.

The model is non-tidal, i.e. deals with tidal averages of observed quantities and with mean flows. The biochemical interaction processes are identical to those used for the Small Coastal Basin models (Hyer and Neilson, 1977).

## II. DESCRIPTION OF STUDY AREA

The tidal portion of the York River watershed has remained relatively rural, with a heavy dependence on farming (chiefly corn and soybeans) and logging. Commercial fishing of oysters, crabs and pelagic fish is also important. Industry is concentrated at both ends of the York. Upstream, at West Point, (see Figure 1) is a pulp and kraft paper mill. Downstream, near the mouth, are an oil refinery and a fossil-fueled electric power plant.

The climate is humid-subtropical. There are approximately 45 inches of rain, of which approximately 12 inches is runoff. Precipitation is lowest between September and January and highest in July and August. Owing to evapotranspiration, however, the heavy thunderstorms of summer have much less effect on fluvial flow than do the rains of spring. Air temperature in January varies from a low of approximately 30°F (-1°C) to a high of 50°F (10°C). In July the mean daily maximum temperature is approximately 88°F (30°C) and the minimum of 68°F (20°C).

The most representative stream gauging stations in the drainage basin are at Hanover, on the Pamunkey and Beulahville on the Mattaponi. The average discharges at these stations are 963 cfs ( $27.3 \text{ m}^3 \text{ sec}^{-1}$ ) and 580 cfs ( $16.4 \text{ m}^3 \text{ sec}^{-1}$ ) respectively. River discharge tends to be greater than average in the period January - April and much less than average in July - September. The gauging station at Hanover has recorded historical extremes of 40,300 cfs ( $1140 \text{ m}^3 \text{ sec}^{-1}$ ) and 12 cfs

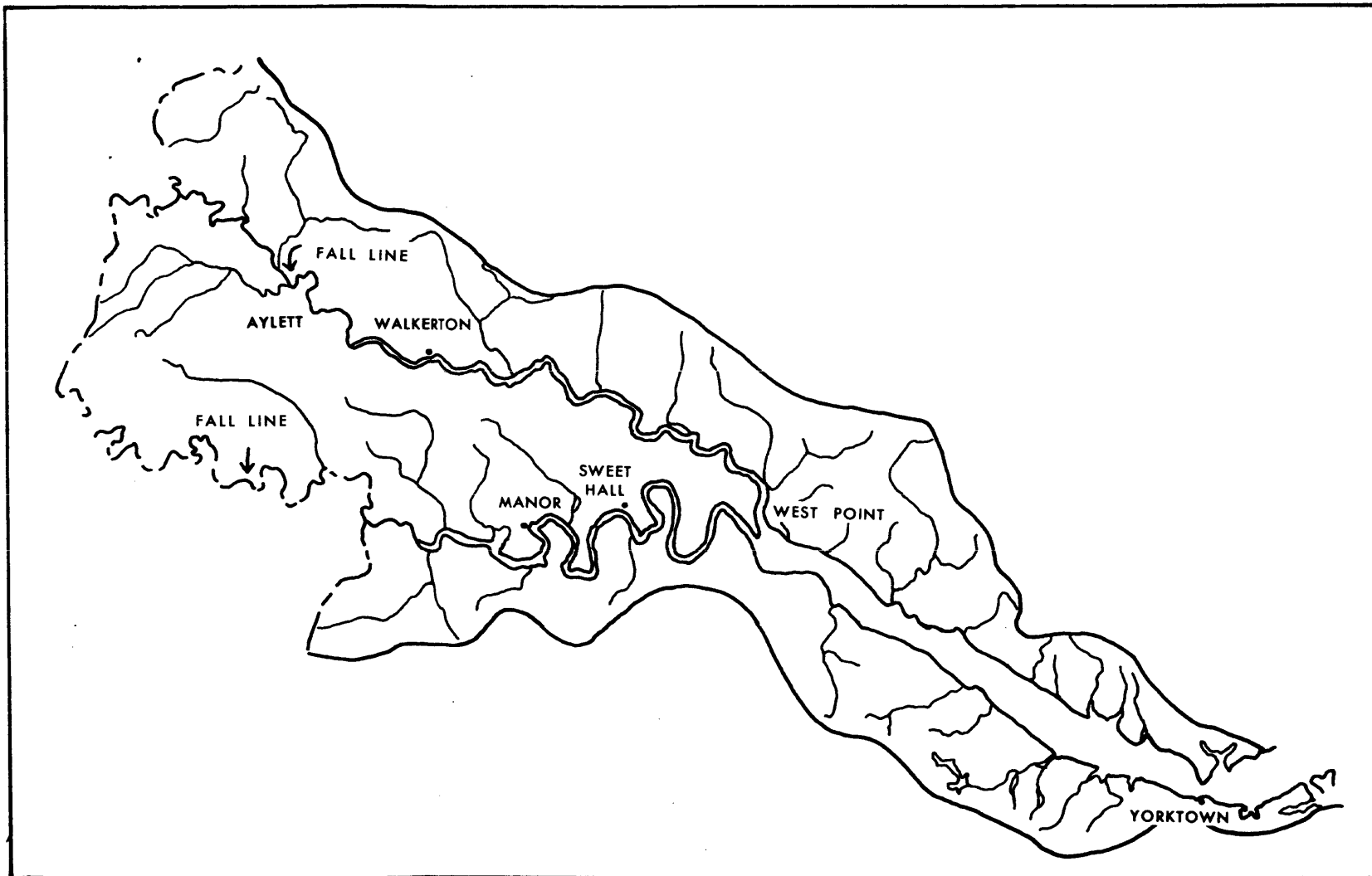


Figure 1. Downstream sub-basin of York drainage basin.

( $0.3 \text{ m}^3 \text{ sec}^{-1}$ ) with extremes at Beulahville of 16,900 cfs ( $479 \text{ m}^3 \text{ sec}^{-1}$ ) and 5.9 cfs ( $0.17 \text{ m}^3 \text{ sec}^{-1}$ ).

Tidal waves propagate upstream at approximately fourteen miles per hour although tidal patterns near the mouth are much more complicated (see Figure 2). As the tidal wave progresses, its amplitude increases. The mean tidal range is 2.2 feet (0.7 m) at Tue Marshes Light and 3.0 feet (0.9 m) at West Point. The tide range continues to increase in the tributaries, reaching 3.9 feet (1.2 m) at Walkerton in the Mattaponi and 3.3 feet (1.0 m) at Northbury in the Pamunkey. Tidal action ceases at the fall line, which is approximately three miles upstream of the Route 360 bridge in both the Mattaponi and Pamunkey Rivers. The tidal wave also undergoes a change in phase relationship. At Tue Marsh, low water occurs only about an hour after maximum ebb current, indicating an almost pure traveling wave. At West Point, this time difference is about two hours, indicating a shift toward standing wave characteristics. Average tidal current increases from 1.0 feet per second (30 cm/sec) near the mouth to 1.8 feet per second (54 cm/sec) near West Point but then decreases to 1.5 feet per second (46 cm/sec) at Walkerton and 0.8 feet per second (24 cm/sec) at Northbury.

Net tidal prism has been calculated from the intertidal volumes of Cronin (1971). Figure 3 shows net tidal prism versus distance upstream for the York. Although monotonic by definition, the tidal prism curves are not linear, but reflect the changes in tidal amplitude and stream geometry as the observer proceeds upstream.

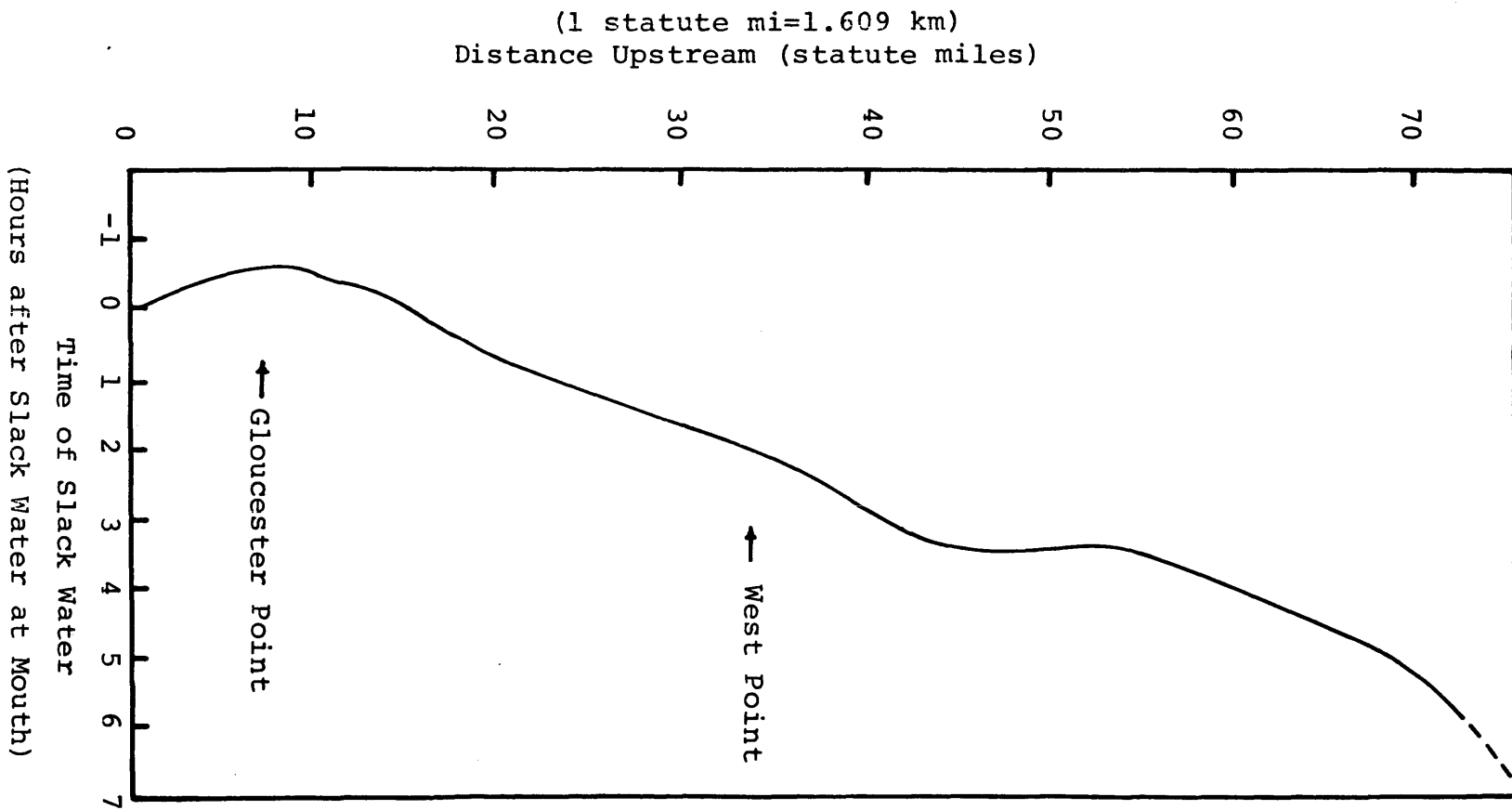


Figure 2. York and Pamunkey time of slack water relative to York River mouth.

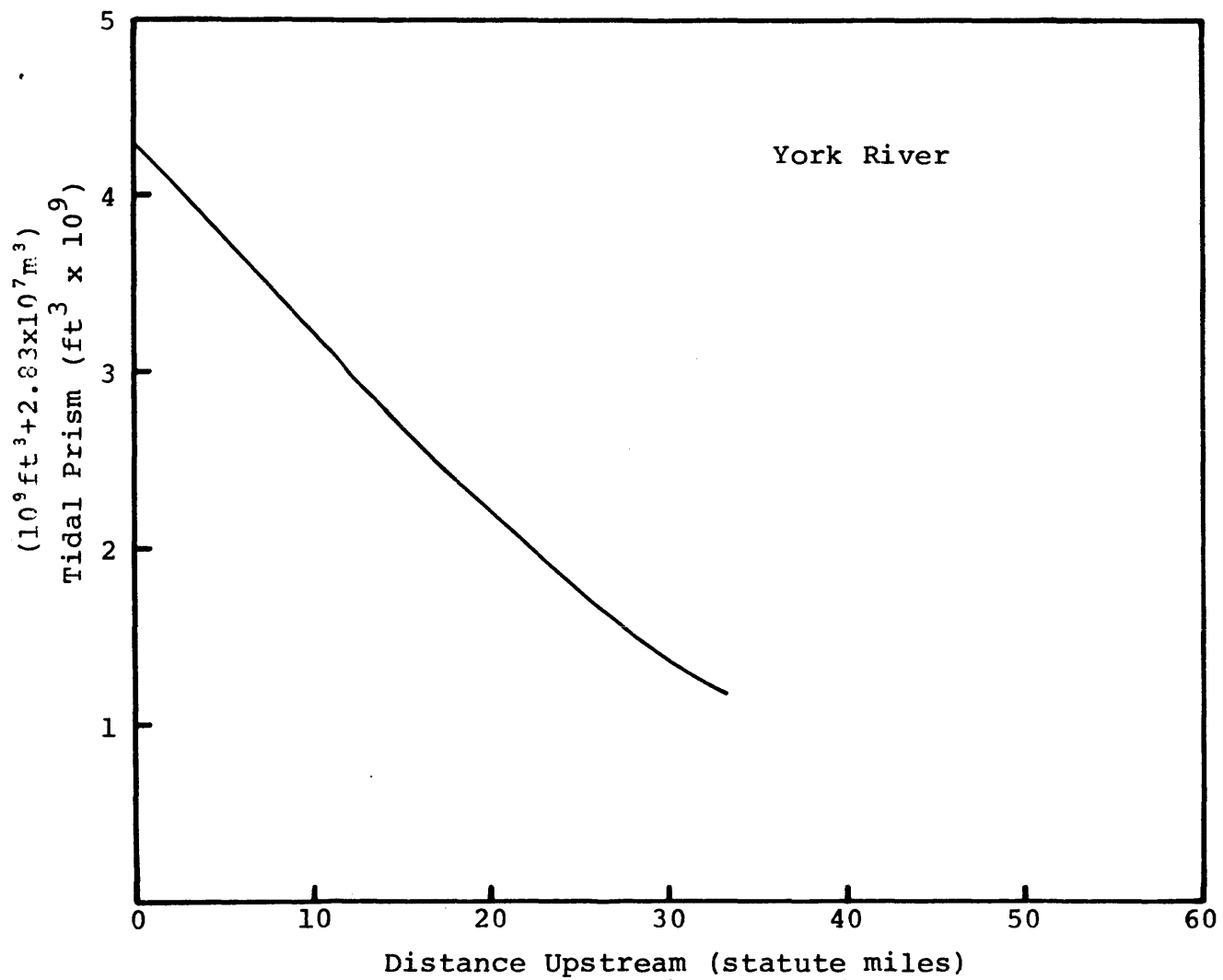


Figure 3. York River calculated tidal prism.  
 1 statute mi=1.609 km

### III. DESCRIPTION OF THE WATER QUALITY MODEL

#### A. Biochemical Interactions

The model has ten components, i.e. ten dependent variables predicted as a function of space and time. Eight of these components interact (see Figure 4), with chlorophyll being the kingpin of the model. There are two closed nutrient cycles which begin and end at chlorophyll (here used as an index of phytoplankton biomass). In addition, the carbonaceous BOD-dissolved oxygen submodel interacts with chlorophyll through photosynthesis and respiration terms and with the nitrogen cycle through an oxidation term. Salinity is independent of the other components (apart from a weak influence on saturation concentration of dissolved oxygen) and bacteria is totally independent of the other components. For a discussion of parameters, see a description of the ecosystem model used for the Back and Poquoson Rivers (Hyer and Neilson, 1977).

#### B. Hydraulic Processes

The model includes the following transport processes: longitudinal mean advection and gravitational circulation; longitudinal dispersion; lateral dispersion; vertical mixing and advection resulting from the gravitational circulation. The theories are given below.

##### 1. Longitudinal.

The freshwater discharge into the first reach is specified, as is the drainage area upstream of the first transect. This flow is partitioned among the

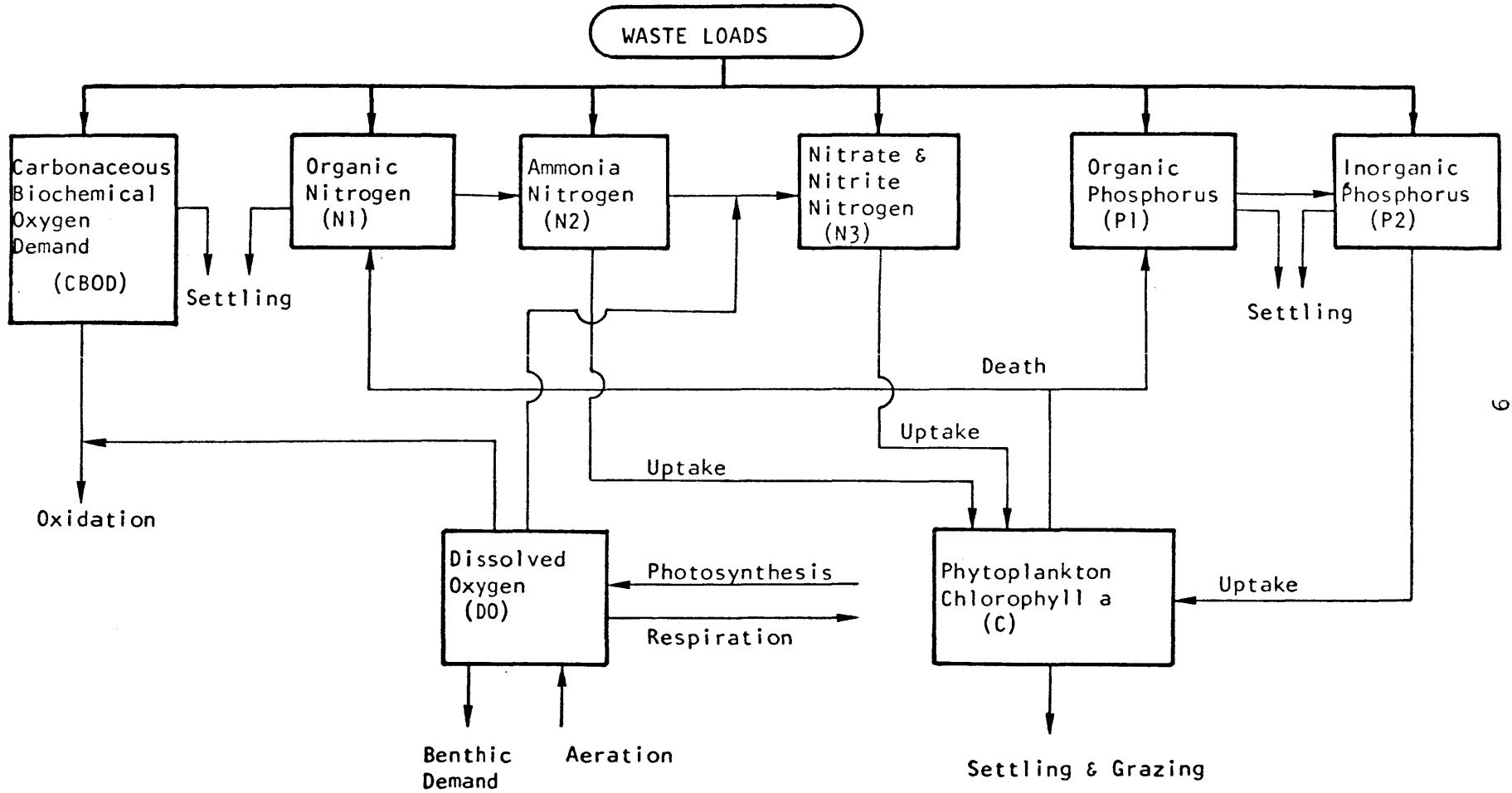


Figure 4. Schematic Diagram of Interaction of Ecosystem Model

six compartments according to partial cross-section areas in the farthest upstream transect. The drainage area of each reach is specified. Lateral inflow into each reach is calculated based on the assumption of equal runoff for equal area (hydrologic homogeneity). One-half of the lateral inflow is assigned to each side lateral division.

The gravitational circulation is driven by the haline structure and the equations used in the model are based on the theory of Hansen and Rattray (1965). They have derived the longitudinal transport in a stratified estuary as a function of depth. In the absence of wind stress, this transport is

$$\phi(\eta) = \frac{1}{2} (2 - 3\eta + \eta^3) + \frac{\nu Ra}{48} (\eta - 3\eta^3 + 2\eta^4)$$

where  $\eta$  is the dimensionless depth and  $\nu Ra$  is a dimensionless parameter describing the intensity of estuarine gravitational circulation. Inspection of the velocity profile curves reveals that the dimensionless level of no motion is very nearly 0.5. However for real (non-rectangular) channels, the transport in the upper layer is:

$$Q_u = Q \left( \frac{11}{16} + \frac{\nu Ra}{192} f(\eta) \right)$$

where  $Q$  is the fresh water inflow and  $f(\eta)$  is a function of the dimensionless depth, to be described under Method of Solution. The transport in the lower layer is then:

$$Q_L = Q - Q_u$$

The quantity  $\nu Ra$  can be calculated from field data. Hansen and Rattray (1966) give the following relation:

$$\nu Ra = 16F_m^{-3/4}, \quad \text{where}$$

$$F_m = U_f / \sqrt{gh\Delta\rho/\rho}, \quad \text{a densimetric}$$

Froude number. The parameter  $F_m$  is calculated empirically for conditions at the mouth of the river. To allow for the streamwise variation of mean flow, the following equation is used:

$$Q_u = \begin{cases} Q \left( \frac{11}{16} + \frac{\nu Ra}{192} f\left(\frac{x}{L}\right) \right) & \text{for } x \leq L \\ \frac{11}{16} Q & \text{for } x > L \end{cases}$$

$f(\theta)$  is derived empirically and  $L$  is the intrusion length.

$$f(0) = 1, \text{ and}$$

$$f(1) = 0.$$

To extrapolate intrusion length from one condition to the general case, a scaling argument is used. According to Hansen and Rattray (1965):

$$L = \frac{QD}{BK_v} \frac{M}{\nu}$$

where  $M$  is a tidal mixing parameter,  $Q$  is fresh water flow,  $D$  is depth and  $B$  is width and  $K_v$  is the vertical turbulent mixing coefficient. From Hansen and Rattray (1966):

$$M_s \propto Q^{-7/5}, \text{ so that}$$

$$L \propto Q^{-2/5}.$$

The functional form of  $f\left(\frac{x}{L}\right)$  was chosen in the process of model calibration to be:

$$f\left(\frac{x}{L}\right) = \sqrt{1 - \frac{x}{L}}; \quad x < L$$

Since gravitational circulation has been included explicitly, the corresponding dispersion coefficient (shear effect) should not be included, as it would have to be in a one-dimensional model. However, since tidal advection does not appear explicitly in the model, the so-called "phase effect" dispersion coefficient (Kuo, in Hyer, et al., 1975, p. 74) must be included. This mode of transport arises out of the combined effect of lateral variation in tidal current strength and lateral mixing. Salt, for example, is carried farther upstream in the center channel than along the shoals, during flood tide. Lateral mixing tends to spread this salt outward, toward the banks, where tidal current is weaker. On the subsequent ebb tide, this salt is not carried back as far as its origin. The net effect is a displacement upstream. This effect is approximated by a dispersion coefficient (Kuo, op. cit., p. 76)

$$E_t = \beta U_t \sqrt{\bar{A}}, \text{ where}$$

$U_t$  is the magnitude of the tidal current,  $\bar{A}$  is the time-average cross-section area and  $\beta$  is an empirical constant of order unity.

## 2. Vertical

Vertical volume transport from the lower layer into the upper is calculated directly from the convergence of the mean flow in the lower layer. The vertical mixing coefficient is estimated by successive trial. Values tend to lie in the range  $10^{-4}$  ft<sup>2</sup>/sec -  $10^{-3}$  ft<sup>2</sup>/sec (0.09 - 0.9 cm<sup>2</sup>/sec).

## 3. Lateral

No lateral advection between compartments occurs in the model. However, lateral mixing is provided for. Holley, Harleman and Fischer (1970) have summarized the results of several previous investigation who have found the lateral dispersion coefficient  $C_y$  to be approximately

$$C_y = 0.067 RU, \text{ where}$$

$R$  is the hydraulic radius and  $U$  is the shear velocity. For the York River estuary, the numerical result is of the order of 5 ft<sup>2</sup>/sec (4500 cm<sup>2</sup>/sec).

## C. Method of Solution

The basic equation given in the previous sections must be put in a form suitable for digital computation. This means expressing the equations in finite-difference form, so that

they may be time-integrated using a digital computer. The water body must be conceptually broken down into control volumes, in each of which the water quality components are spatially averaged. Thus, the set of equations to be solved per time step is the product of the number of control volumes (model compartments) times the number of components being modeled.

Each compartment exchanges material with the one above it or below it, with the one or two components beside it and with the compartments upstream and downstream from it. In generating the equations, each of these exchange rates must be expressed in terms of compartmental averages, a process necessarily involving approximations. Let a component  $C$  be in the  $i$ th reach,  $j$ th position laterally and the  $r$ th layer be represented by

$$C_{i,j,r}$$

In the quasi-three dimensional York model:

$$1 \leq i \leq 20 \text{ (} i = 1 \text{ at upstream end)}$$

$$\left\{ \begin{array}{l} j = 1 \text{ for south and west side} \\ j = 2 \text{ for center} \\ j = 3 \text{ for north and east side} \end{array} \right.$$

$$\left\{ \begin{array}{l} r = 1 \text{ for upper layer} \\ r = 2 \text{ for lower layer} \end{array} \right.$$

The lateral flux into the  $i, j, r$  compartment from the  $i, j-1, r$  compartment is

$$\frac{(C_{i,j-1,r} - C_{i,j,r})}{W_{i,j-1,r}} L_{i,j-1,r} E_{i,j-1,r} \quad \text{where}$$

$L_i$  is the length of the  $i$ th segment,  $H_{i,j-1}$  is the depth of the interface between the  $i, j-1, r$  compartment and the  $i, j, r$  compartment and  $W_{i,j-1,r}$  is the center-to-center distance.  $E_{i,j-1}$  is the mixing coefficient between these two compartments. Naturally the mass balance for the  $i, j-1, r$  compartment has a corresponding efflux.

There is both mixing and advection longitudinally. The transport into the  $i, j, r$  compartment from the  $i, j-1, r$  compartment is

$$\frac{(C_{i,j-1,r} - C_{i,j,r})}{X_{i-1} - X_i} A_{i,j,r} E_{i,j}^1 \quad \text{where}$$

$X$  is the distance upstream of the center of the  $i$ th segment,  $A_{i,j,r}$  is the interface area between the  $i, j-1, r$  compartment and the  $i, j, r$  compartment and  $E_{i-j}^1$  is the mixing coefficient between the two compartments.

Advection transport includes the two-layer estuarine flow. Let the total mean fresh water flow into the  $i, j, 1$  compartment and the  $i, j, 2$  compartment be:

$$(Q_m)_{i,j}$$

Hansen and Rattray (1965) give the transport function for gravitational circulation as

$$Q(\eta) = \frac{1}{2} (2 - 3\eta + \eta^3) - \frac{\nu Ra}{192} (4\eta - 12\eta^3 + 8\eta^4),$$

where  $\nu Ra$  is a parameter expressing the strength of gravitational circulation and  $\eta$  is the dimensionless depth. This transport function can be written

$$Q(n) = P_1(n) - \frac{\nu Ra}{192} P_2(n)$$

The flow into the upper (i.e.  $i, j, 1$ ) compartment is:

$$Q_{i,j,1} = (Q_m)_{i,j} \left( \frac{1 - P_1\left(\frac{Z_i}{H}\right) + \frac{\nu Ra}{192} P_2\left(\frac{Z_i}{H}\right) F\left(\frac{X_i}{L}\right)}{1 - P_1\left(\frac{H_j}{H}\right) + \frac{\nu Ra}{192} P_2\left(\frac{H_j}{H}\right) F\left(\frac{X_i}{L}\right)} \right)$$

where:  $Z_i$  = depth from surface to interface between upper and lower layer;

$H_j$  = total depth of upper and lower  $j$ th compartments combined;

$H$  =  $\max(H_1, H_2, H_3)$ ;

$$F\left(\frac{X}{L}\right) = \begin{cases} \sqrt{1 - \frac{X}{L}} & x \leq L \\ 0 & x > L \end{cases}$$

$L$  = length scale for circulation.

Both  $Z_i$  and  $L$  are determined empirically. The flow into the lower compartment is:

$$Q_{i,j,2} = (Q_m)_{i,j} - Q_{i,j,1}$$

There is both advective transport and turbulent mixing between the upper and lower layers. The advective transport comes from the convergence of the flow in the lower layer, i.e.

$$q_{i,j} = Q_{i,j,2} - Q_{i+1,j,2}$$

The transport rate into the upper layer due to vertical mixing is:

$$\frac{C_{i,j,2} - C_{i,j,1}}{D_{i,j}} L_i W_i E_{i,j}^{11}, \quad \text{where}$$

$D_{i,j}$  is the vertical separation of the centers of the upper

and lower compartments,  $W_i$  is the width of the interface and  $E_{i,j}^{11}$  is the mixing coefficient.

The integration scheme uses an implicit method for the biochemical terms and the longitudinal exchanges while calculating the lateral and vertical exchanges explicitly at the back time step. The finite difference equation for time step beginning at time  $t$  can be written:

$$\begin{aligned} \frac{C_{i,j,e}^{t+\Delta t} - C_{i,j,e}^t}{\Delta t} = & \frac{1}{2}(\alpha^t C_{i-1,j,e}^t + \beta^t C_{i+1,j,e}^t + \Gamma C_{i,j,e}^t \\ & + \alpha^{t+\Delta t} C_{i-1,j,e}^{t+\Delta t} + \beta^{t+\Delta t} C_{i+1,j,e}^{t+\Delta t} \\ & + \Gamma^{t+\Delta t} C_{i,j,e}^{t+\Delta t}) + \epsilon^t (C_{i,j-1,e}^t - C_{i,j,e}^t) \\ & + \mu^t (C_{i,j+1,e}^t - C_{i,j,e}^t) \\ & + \nu^t (C_{i,j,3-e}^t - C_{i,j,e}^t) + J_{i,j,e}^t \end{aligned}$$

where  $\alpha$ ,  $\beta$ ,  $\Gamma$ ,  $\epsilon$ ,  $\mu$  and  $\nu$  are (possibly time-dependent) known expressions and  $J$  is the source term, including both external loadings and transmutations from other components. The factor  $\Gamma$  includes the first-order decay rate, if any. If all the terms containing  $t+\Delta t$  (i.e. the quantities yet unknown at time  $t$ ) are isolated on one side of the equation, the result is:

$$\begin{aligned} C_{i,j,e}^{t+\Delta t} (1 - \frac{\Gamma^{t+\Delta t} \Delta t}{2}) - C_{i-1,j,e}^t \frac{\alpha^{t+\Delta t} \Delta t}{2} \\ - C_{i+1,j,e}^{t+\Delta t} \frac{\beta^{t+\Delta t} \Delta t}{2} \\ = C_{i,j,e}^t (1 + \frac{\Gamma^t \Delta t}{2}) + C_{i-1,j,e}^t \frac{\alpha^t \Delta t}{2} \end{aligned}$$

$$\begin{aligned}
& + C_{i+1,j,e}^t \frac{\beta \Delta t}{2} + (C_{i,j+1,e}^t - C_{i,j,e}^t) \mu \Delta t \\
& + (C_{i,j-1,e}^t - C_{i,j,e}^t) \epsilon \Delta t \\
& + (C_{i,j,3-e}^t - C_{i,j,e}^t) \nu \Delta t + J_{i,j,e}^t
\end{aligned}$$

The unknown on the left-hand side of the equation are interconnected and must be solved simultaneously. This kind of system of equations is called "tridiagonal" due to the pattern made when the equations are expressed in matrix form. The special fast method for solving this kind of system is found elsewhere (e.g. Fang, et al., 1973).

#### D. Evaluation of Parameters and Rate Constants

##### 1. Hydraulic Inputs

a. Fresh-water Inflow. The York is formed by the confluence of the Mattaponi and Pamunkey Rivers. Both of these streams are gauged; the Mattaponi at Beulahville and the Pamunkey at Hanover (see Figure 1). The records for these gauging stations for the months of June through September, 1976, are shown in Table 1. For model operation these flows were averaged for the month period prior to the day on which the survey was conducted and were augmented to include the lateral inflow occurring between the gauging station and the transect farthest upstream. Finally, the Mattaponi flow went into the J=3 compartment while the Pamunkey flow was divided equally between the J=1 and J=2 compartments.

b. Longitudinal Dispersion Coefficient. The formula used is given in a previous section. The constant  $\beta$  was found to give the best results when set at 2. The dispersion

TABLE 1. Flow\* Records for Beulahville  
and Hanover, Virginia, 1976

Date	Beulahville (Mattaponi)				Hanover (Pamunkey)			
	June	July	Aug.	Sept.	June	July	Aug.	Sept.
1	367	260	110	58	860	257	151	174
2	369	190	90	53	1020	246	154	187
3	401	160	72	62	1080	237	153	187
4	467	140	60	67	1010	224	148	183
5	442	120	56	66	641	219	137	162
6	358	120	50	57	475	202	134	150
7	297	130	46	49	366	210	129	147
8	258	160	47	45	349	226	125	151
9	237	190	123	41	325	221	246	151
10	200	190	249	43	305	244	269	150
11	179	170	207	65	289	256	226	136
12	163	180	131	61	259	265	183	120
13	155	160	91	52	248	259	159	109
14	145	150	74	46	263	237	168	110
15	142	140	123	48	285	224	180	119
16	137	120	188	385	277	261	598	521
17	154	150	176	836	329	305	501	627
18	203	240	171	1010	468	257	281	413
19	216	420	133	878	612	223	208	321
20	245	250	100	585	581	223	175	267
21	311	160	81	371	597	210	160	193
22	292	130	69	247	893	198	146	159
23	277	110	61	187	1790	182	143	141
24	287	95	55	148	1240	177	129	140
25	293	90	50	123	830	168	124	143
26	367	80	47	109	820	165	112	148
27	473	78	43	107	1470	177	112	179
28	510	76	49	314	665	169	124	830
29	429	78	64	340	299	160	154	579
30	342	110	69	273	259	162	165	329
31	---	140	65	---	---	159	171	---
Min.	137	76	43	41	248	159	112	109
Mean	291	154	95.2	224	630	217	189	241
Max.	510	420	249	1010	1790	305	598	830

\* All flows given in cubic feet per second.

coefficient then turns out to be in the range 500-1000 ft<sup>2</sup>/sec.

c. Circulation Parameter. The input constant  $\nu Ra$  indicates the strength of the density-induced circulation. This parameter and the input  $\beta$  were simultaneously adjusted to reproduce the observed salinity. The final value of  $\nu Ra$  was 100.

## 2. Biochemical Inputs.

a. Reaeration Coefficient  $k_2$ . O'Connor and Dobbins (1956) presented a theoretical derivation of the reaeration coefficient, in which fundamental turbulence parameters were taken into account. They derived the following formula:

$$(k_2)_{20} = \frac{(D_c U)^{1/2}}{H^{3/2}}$$

where  $D_c$  is the molecular diffusivity of oxygen in water,  $U$  and  $H$  are the cross-sectional mean velocity and depth respectively, and  $(k_2)_{20}$  is the reaeration coefficient at 20°C. This formula has been shown to give a satisfactory estimate of  $k_2$  for a reach of river with cross-sectional mean depth and velocity more or less uniform throughout the reach. However, this formula must be modified when dealing with two layered systems. The factor  $H^{3/2}$  appearing in the denominator must be broken into two factors.

$$H^{3/2} = H_s^{1/2} H_v, \text{ where}$$

$H_v$  is the mean depth of the volume to which oxygen is being replenished. In the two layered model  $H_v = H_1$ , i.e., the mean

depth of the upper layer. The other depth,  $H_s$  is the characteristic depth of the vertical shear of the horizontal flow.

This depth will have an intermediate value between the depth of the upper layer and the total depth. Hence,

$$H_s = H_1 + 0.5 H_2,$$

i.e., the depth of the upper layer plus half the depth of the lower layer, will be approximately correct.

To adjust  $k_2$  for temperatures other than 20°C, Elmore and West's (1961) formula is used

$$k_2 = (k_2)_{20} \cdot 1.024^{(T-20)}$$

where T is the water temperature in centigrade degrees.

b. CBOD Oxidation Rate,  $k_1$ . The oxidation rate of CBOD (carbonaceous biochemical oxygen demand) normally ranges from 0.1 to 0.5 per day. The rate also depends on water temperature; the following formula is used for this temperature dependence,

$$k_1 = (k_1)_{20} \cdot 1.047^{(T-20)}$$

c. Saturated Oxygen Content,  $DO_s$ . The saturation concentration of dissolved oxygen depends on temperature and salinity. From tables of saturation concentration (Carritt and Green, 1967) a polynomial equation was determined by a least-squares method.

$$DO_s = 14.6244 - 0.367134T + 0.0044972T^2 \\ - 0.0966S + 0.00205TS + 0.0002739S^2$$

where  $S$  is salinity in parts per thousand and  $DO_s$  is in mg/liter.

d. Benthic Oxygen Demand, BEN. The bottom sediment of an estuary may vary from deep deposits of sewage or industrial waste origin to relatively shallow deposits of natural material of plant origin and finally to clean rock and sand. The oxygen consumption rate of the bottom deposits must be determined with field measurements. Field data were obtained in the summer of 1976 (see Table 2). Sampling locations are shown in Figure 5. A value of  $1.0 \text{ gm/m}^2/\text{day}$  at  $20^\circ\text{C}$  is typical average for most estuaries. The temperature effect was simulated by thomann, 1972.

$$\text{BEN} = (\text{BEN})_{20} \cdot 1.065^{(T-20)}$$

where  $(\text{BEN})_{20}$  is the benthic demand at  $20^\circ\text{C}$ .

e. Coliform Bacteria Dieoff Rate,  $k_b$ .

$$k_b = (k_b)_{20} \cdot 1.040^{(T-20)}$$

where  $(k_b)_{20}$  is the dieoff rate at  $20^\circ\text{C}$  and  $T$  is temperature in degrees centigrade. The normal range of  $(k_b)_{20}$  is 0.5-4.0/day.

f. Settling Rate of Organic Nitrogen,  $k_{n11}$ .

$k_{n11}$  is of order of 0.1/day

g. Organic N to  $\text{NH}_3$  Hydrolysis Rate,  $k_{n12}$ .

$$k_{n12} = aT$$

TABLE 2. Benthic Oxygen Demand Studies  
York River, 1976

Date	Station	Benthic Oxygen Demand (gm/m <sup>2</sup> /day)
25 June	7A	1.6
25 June	7B	3.4
2 July	5A	1.5
2 July	1B	0.9

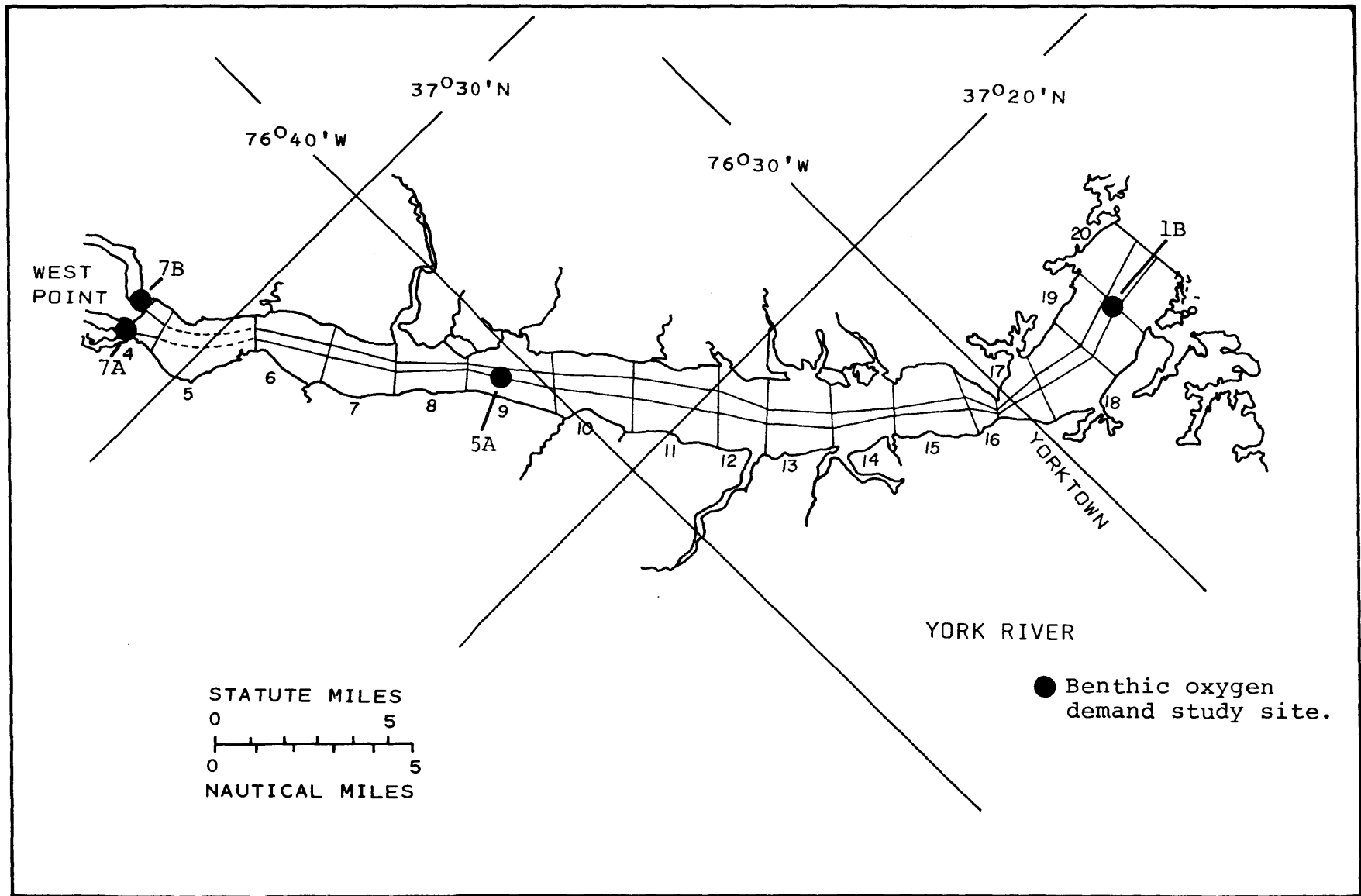


Figure 5. The York River showing model segments and benthic oxygen demand sampling sites.

where  $a$  is of order of 0.007/day/degree.

h.  $\text{NH}_3$  to  $\text{NO}_3$  Nitrification Rate,  $k_{n23}$

$$k_{n23} = aT$$

where  $a$  is of order of 0.01/day/degree.

i.  $\text{NO}_3$  Escaping Rate,  $k_{n33}$

$k_{n33}$  is usually negligible.

j. Organic Phosphorus Settling Rate,  $k_{p11}$

$k_{p11}$  is order of 0.1/day.

k. Organic P to Inorganic P Conversion Rate,  $k_{p12}$

$$k_{p12} = aT$$

where  $a$  is of order of 0.007/day/degree.

l. Inorganic Phosphorus Settling Rate,  $k_{p22}$

$k_{p22}$  is of order of 0.1/day.

m. Nitrogen-chlorophyll Ratio,  $a_n$

$a_n$  is of order of 0.01 mg N/ $\mu\text{g}$  C.

n. Phosphorus-chlorophyll Ratio,  $a_p$

$a_p$  is of order of 0.001 mg P/ $\mu\text{g}$  C.

o. Carbon-chlorophyll Ratio,  $a_c$

$a_c$  is of order of 0.05 mg carbon/ $\mu\text{g}$  C.

p. Oxygen Produced Per Unit of Chlorophyll Growth,  $a_d$

$$a_d = 2.67 \cdot a_c \cdot PQ$$

where PQ is photosynthesis quotient,  $PQ = 1 \sim 1.4$ .

q. Oxygen Consumed Per Unit of Chlorophyll Respired,  
 $a_r$

$$a_r = 2.67 \cdot a_c / RQ$$

where RQ is respiration ratio.

r. Phytoplankton Settling Rate,  $k_{CS}$

$$k_{CS} = S_\ell / h$$

where  $S_\ell$  is settling velocity, whose normal range is 15 to 150 cm/day (0.5 to 5 ft/day).

s. Zooplankton Grazing, Kg. In reality, Kg should depend solely on the concentration of herbivorous zooplankton biomass. This effect has been included in the grazing rate.

t. Endogenous Respiration Rate,  $R_s$

$$R_s = aT$$

where a is of order of 0.005/day/degree.

u. Growth Rate,  $G_c$ . The growth rate expression is that developed by Di Toro, O'Connor and Thomann (1971) and as used in this model is given by

$$G_c = k_{gr} T \cdot I (I_a, I_s, k_e, C, h) \cdot N (N_2, N_3, P_2)$$

temperature effect	light effect	nutrient effect
-----------------------	-----------------	--------------------

where  $k_{gr}$  is the optimum growth rate of the order of 0.1/day/degree. The functional form, I, for the light effect incorporates

vertical extinction of solar radiation and self-shading effect.

The form is

$$I = \frac{2.718}{k_e h} (e^{-\alpha_1 l} - e^{-\alpha_0 l})$$

$$k_e = k_e' + 0.0088 \cdot C + 0.054 \cdot C^{0.66}$$

$$\alpha_1 = \frac{I_a}{I_s} e^{-k_e h}$$

$$\alpha_0 = \frac{I_a}{I_s}$$

$k_e'$  is the light extinction coefficient at zero chlorophyll concentration,  $k_e$  is the overall light extinction coefficient,  $I_a$  is the incoming solar radiation and  $I_s$  is the optimum light intensity, about 300 langley's per day. The nutrient effect makes use of product Michaelis - Menton kinetics and is given by

$$N = \frac{N_2 + N_3}{K_{mn} + N_2 + N_3} \cdot \frac{P_2}{K_{mp} + P_2}$$

where  $K_{mn}$  is the half saturation concentration for total inorganic nitrogen and  $K_{mp}$  is the half saturation concentration for phosphorus.  $K_{mn}$  and  $K_{mp}$  have been reported to be about 0.3 - 0.4 and 0.03 - 0.05 mg/l respectively, although  $K_{mn}$  has been reported as low as 0.008 mg/l and  $K_{mp}$  has been reported as low as 0.015 mg/l.

#### IV. MODEL CALIBRATION AND VERIFICATION

##### A. Calibration Procedure

Before a model can be applied to future predictions, it must be tested and proved capable of reproducing actually observed conditions. Many input constants will be modified in this successive approximation process. These constants are ones that have not been measured directly, but only approximated from existing literature. When one set of field data has been predicted by the model, the model is said to be calibrated. The next step is to keep the same set of input constants and attempt to reproduce a second set of field data. Once this has been done successfully, the model is said to be verified. When verification is first attempted, there is normally a need to readjust some inputs in order to improve the verification without compromising the calibration.

The York ecosystem model was calibrated according to field data collected June 15-16 and July 1-2, 1976. Since manpower and boats were limited and the area to be studied large, the river was covered in two parts. Model segmentation is shown in Figure 5. The calibration results for the center channel are shown in Figures 6 to 15. Part of the point source data was supplied by Betz Engineers through the Hampton Roads Water Quality Agency. The rest came from data compiled by the Water Control Board and used in the calibration of an earlier model (Hyer, et al., 1975). Point source data are shown in Table 3. Nonpoint source loadings from land runoff were provided by Malcolm Pirnie, Inc., through the Hampton Roads Water Quality Agency. The discontinuity in model predictions results from

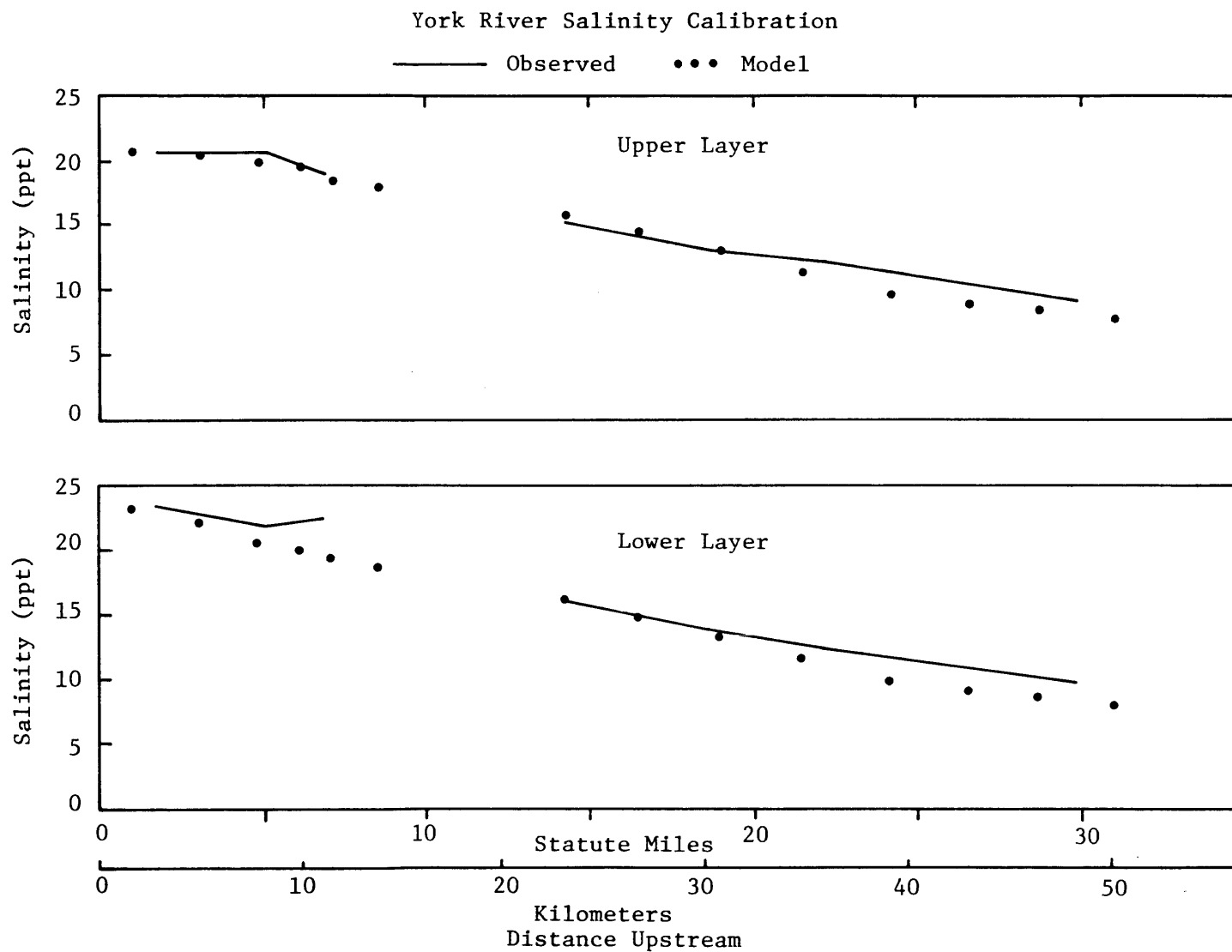


Figure 6. Comparison of calibration results with field observations of salinity.

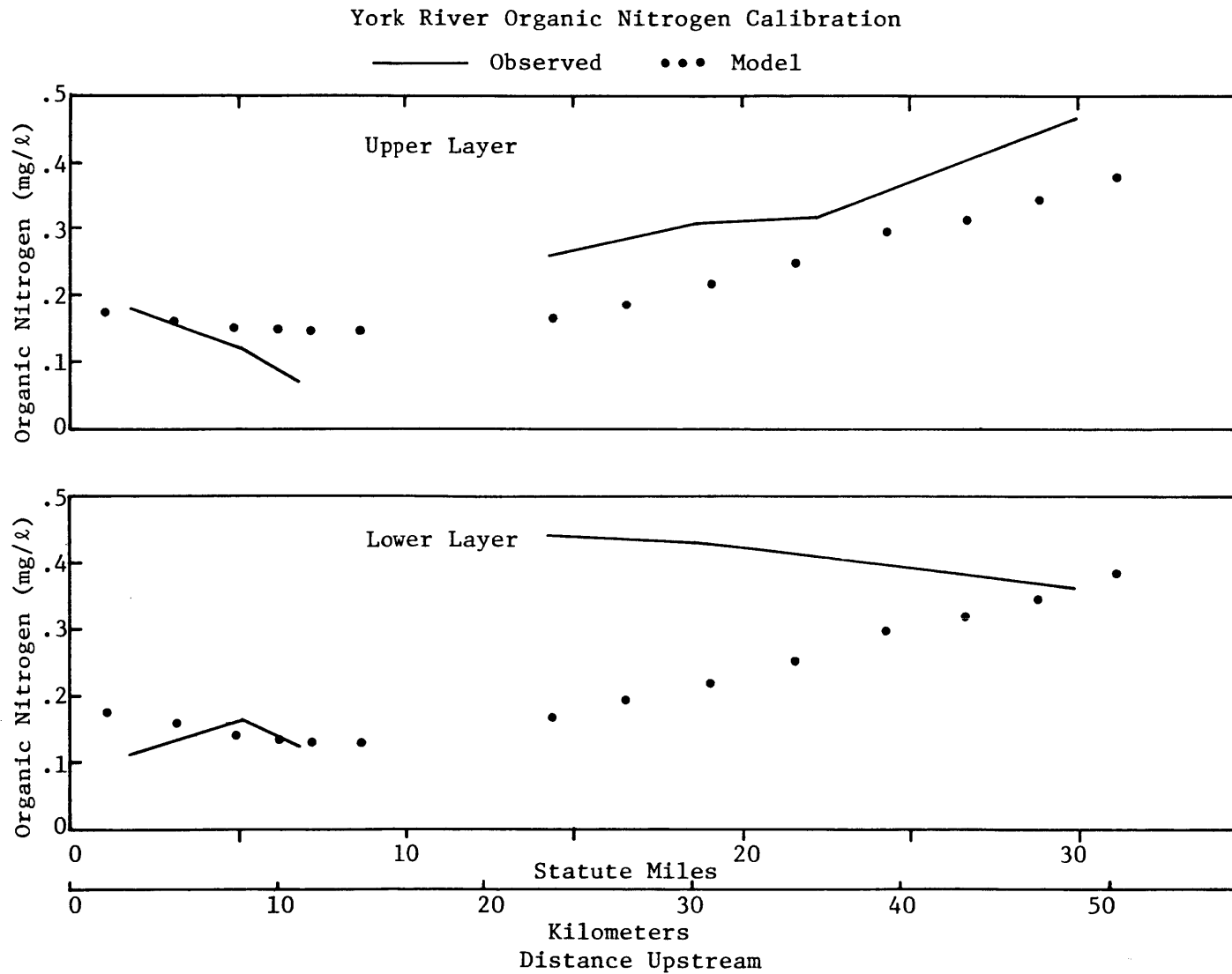


Figure 7. Comparison of calibration results with field observations of organic nitrogen.

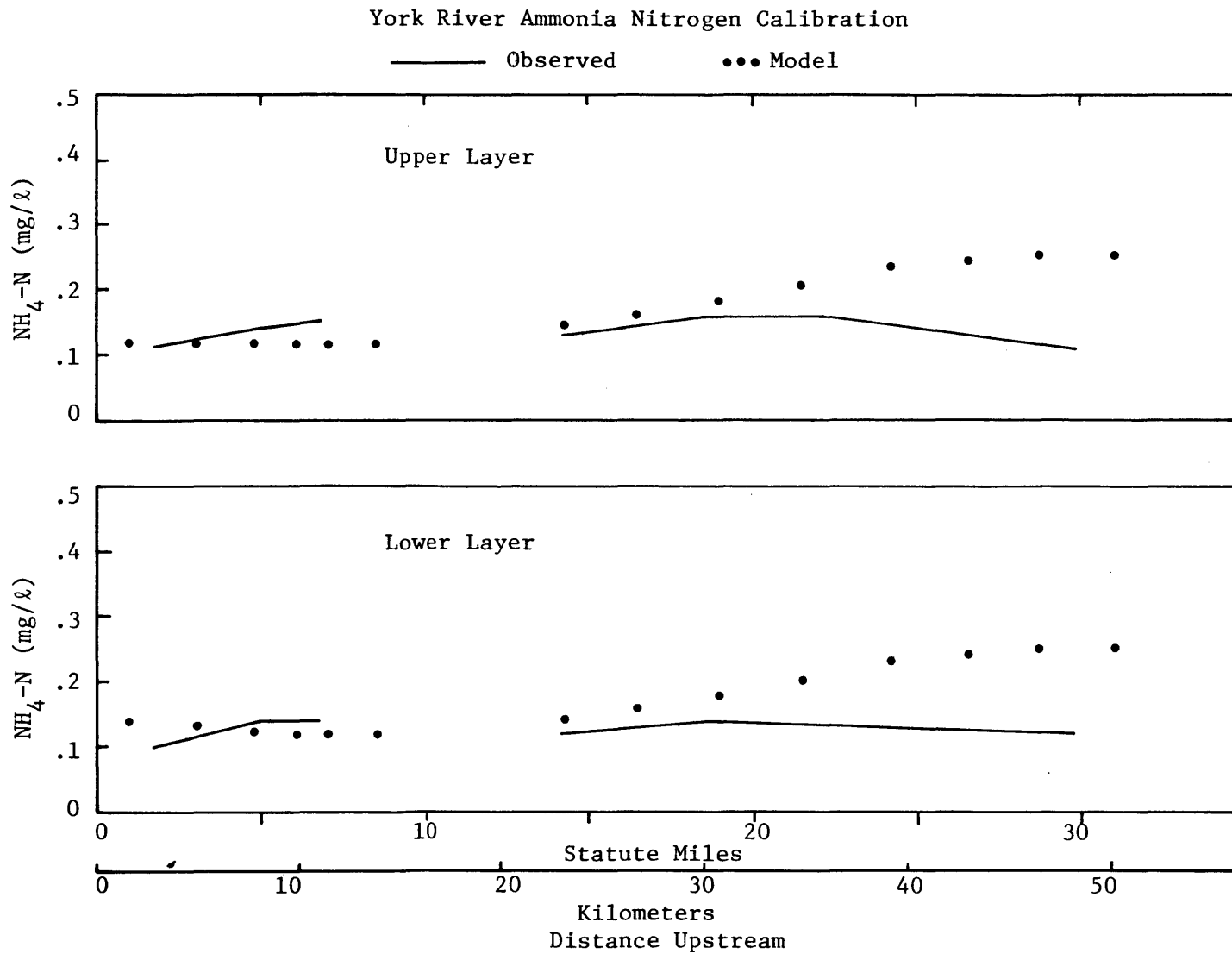


Figure 8. Comparison of calibration results with field observations of ammonia nitrogen.

York River Nitrate plus Nitrite Calibration

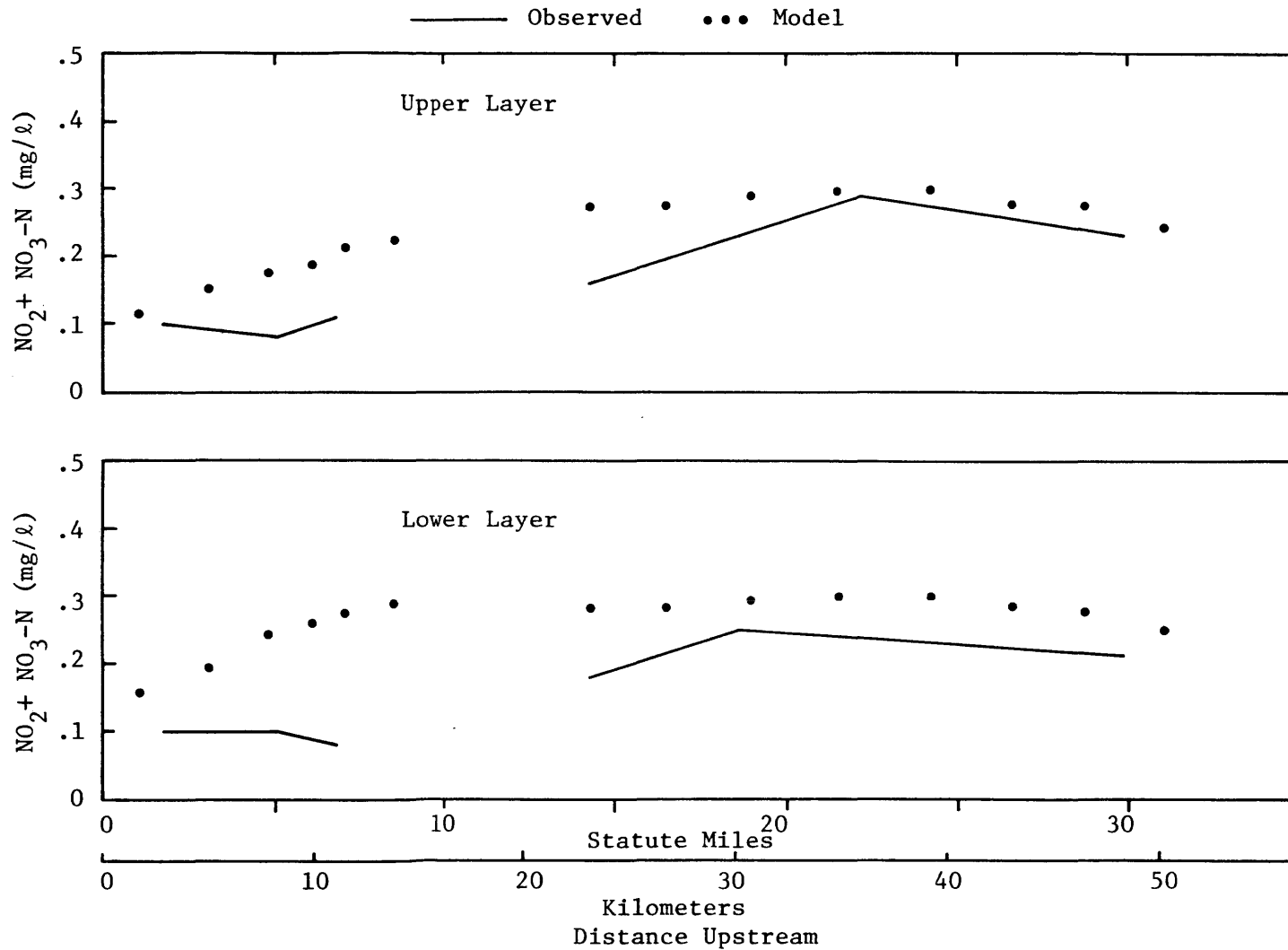


Figure 9. Comparison of calibration results with field observations of nitrite-nitrate nitrogen.

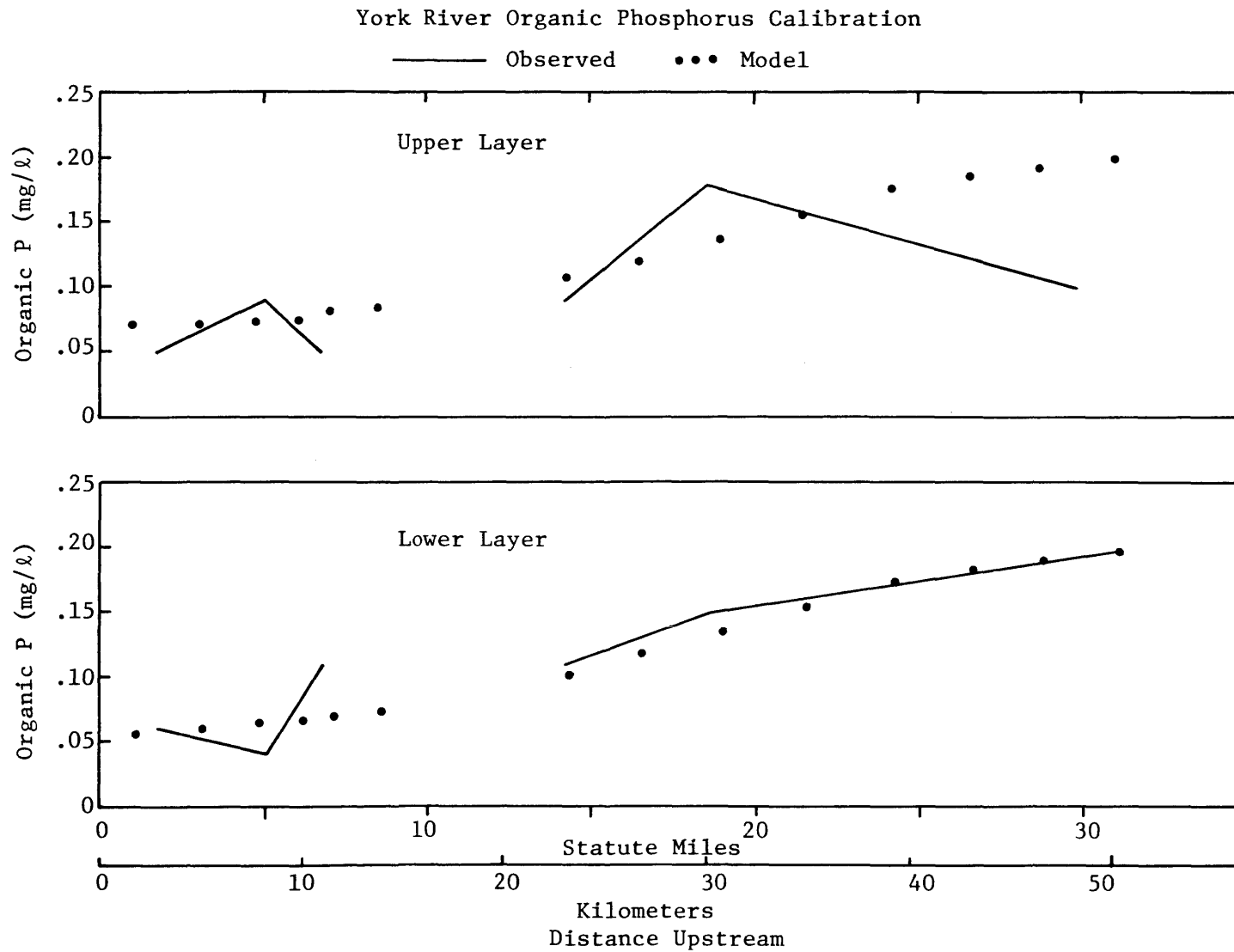


Figure 10. Comparison of calibration results with field observations of organic phosphorus.

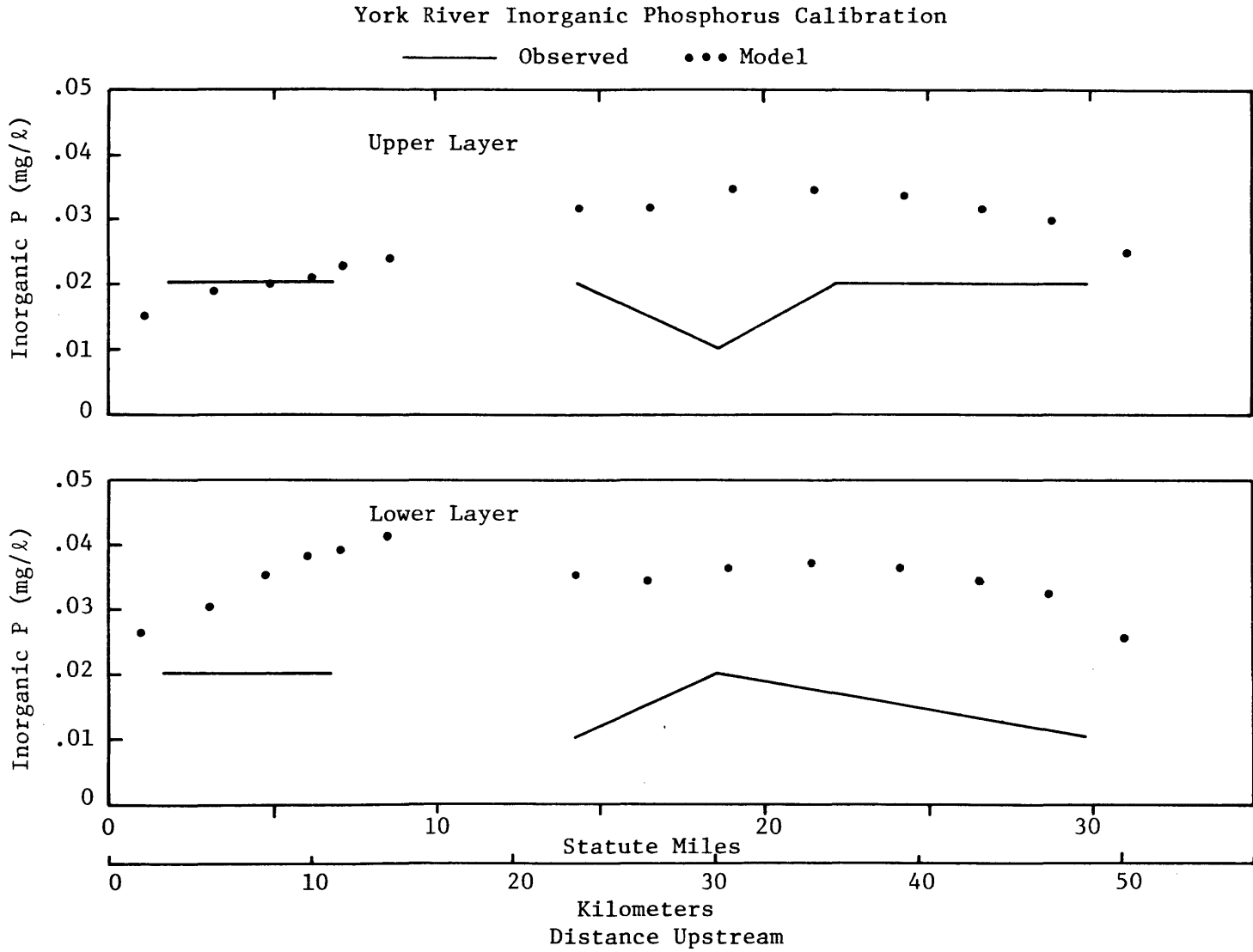


Figure 11. Comparison of calibration results with field observations of inorganic phosphorus.

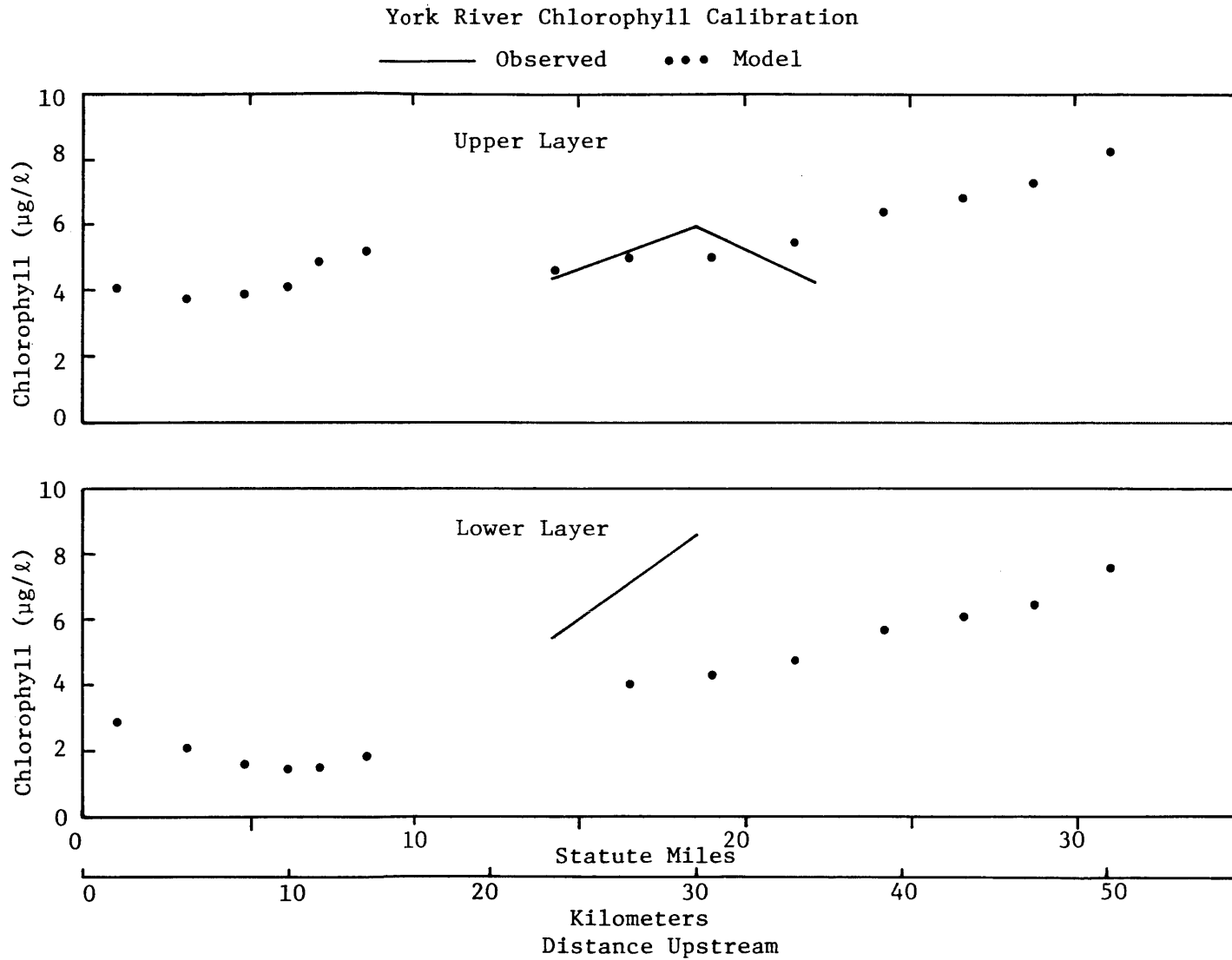


Figure 12. Comparison of calibration results with field observations of chlorophyll.

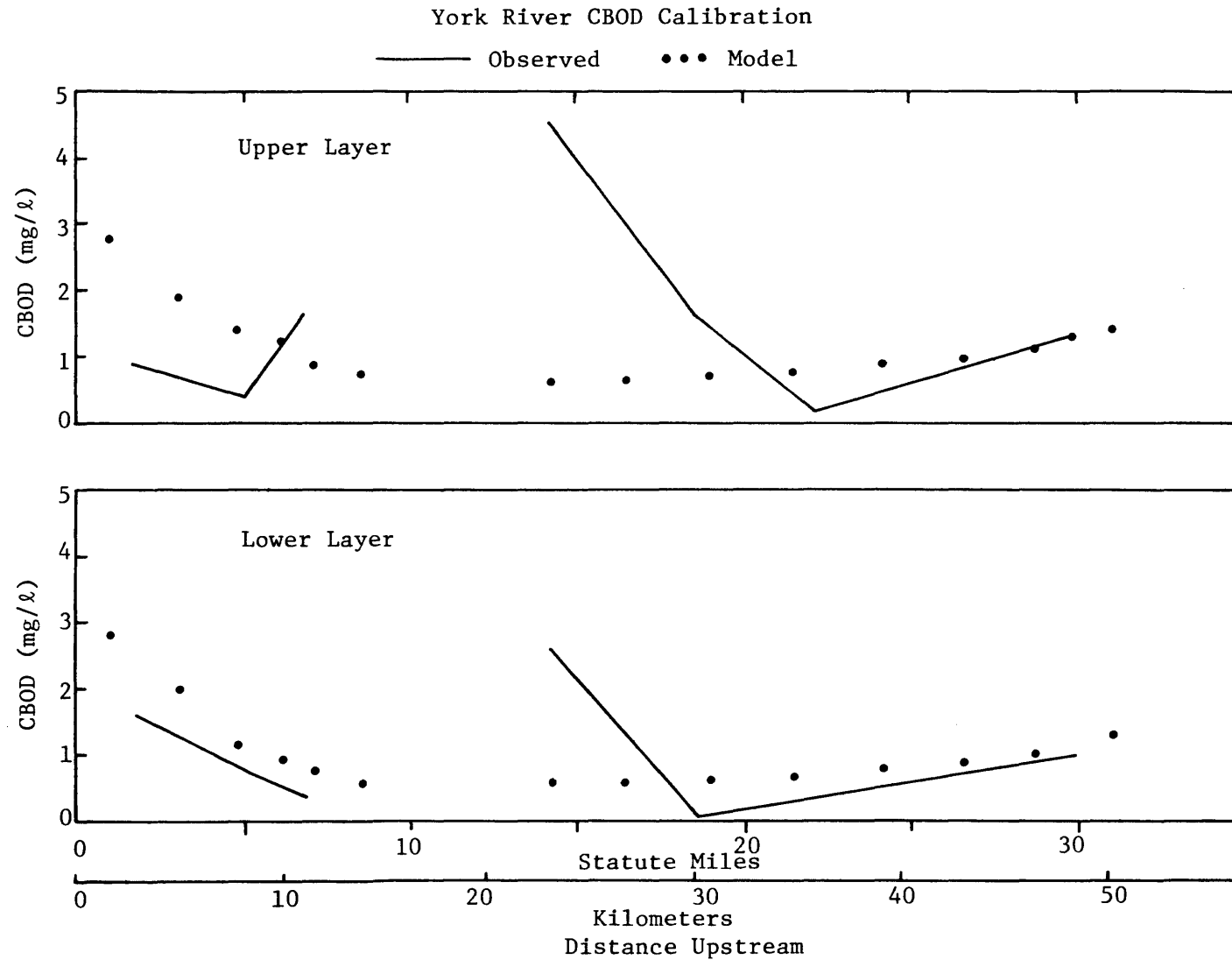


Figure 13. Comparison of calibration results with field observations of CBOD.

### York River Dissolved Oxygen Calibration

— Observed    ••• Model

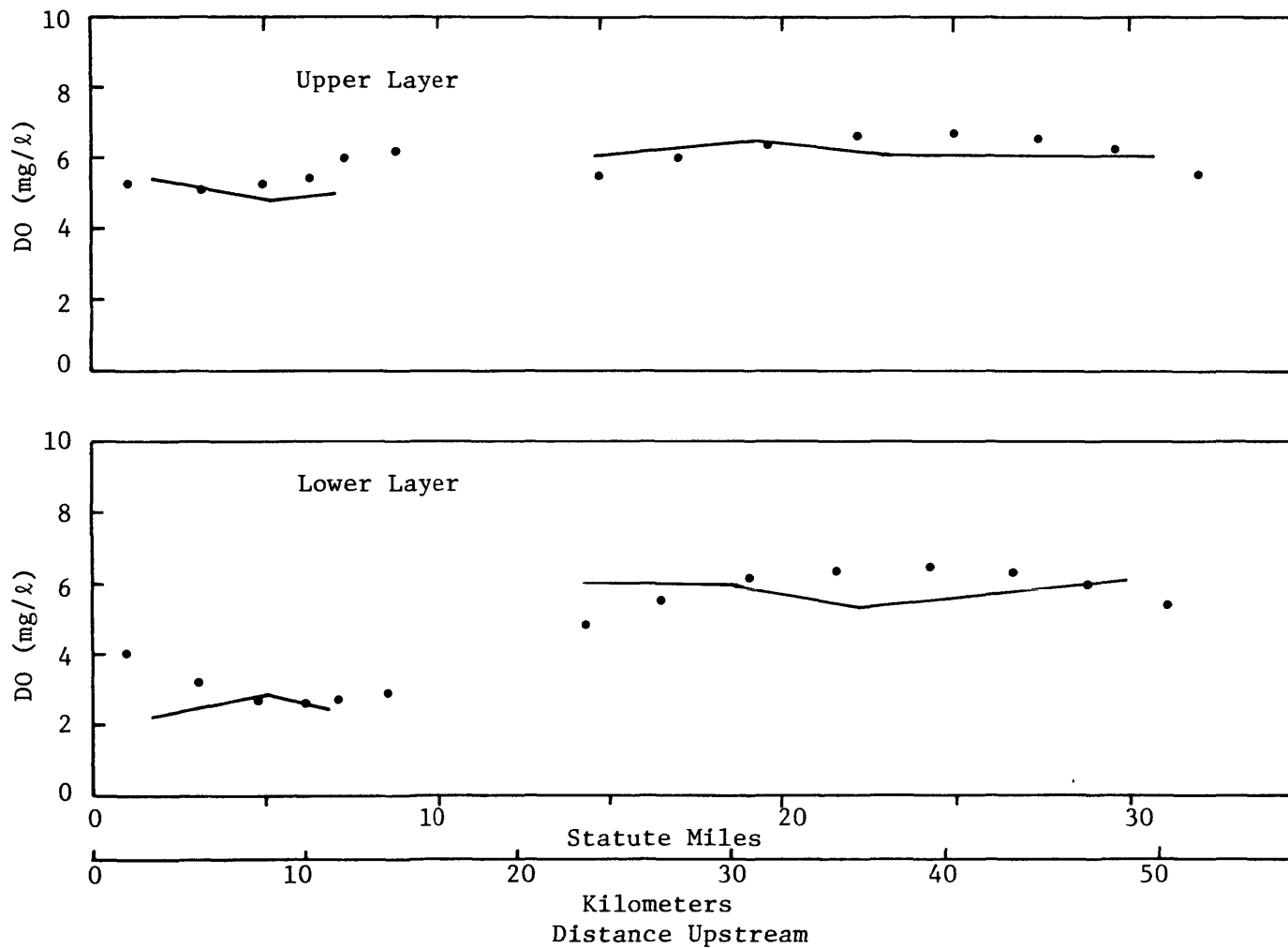


Figure 14. Comparison of calibration results with field observations of dissolved oxygen.

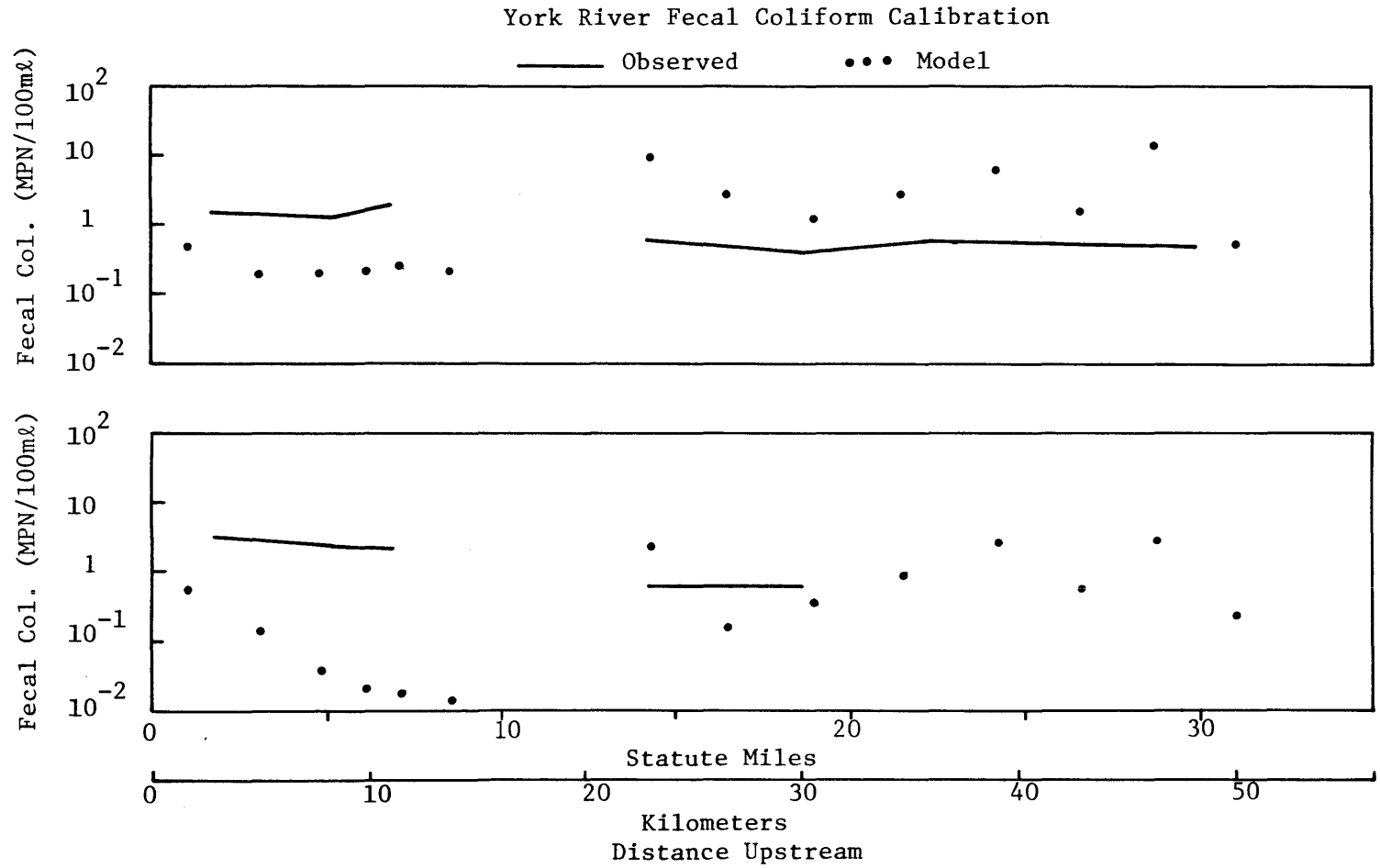


Figure 15. Comparison of calibration results with field observations of fecal coliform.

TABLE 3. Point Sources of Loading Used in Calibration and Verification

Name	Lateral Segment Number	Longitudinal Segment Number	Flow (cfs)	BOD <sub>5</sub> (lb/day)	Organic N (lb/day)	Ammonia (lb/day)	NO <sub>2</sub> and NO <sub>3</sub> (lb/day)	Organic P (lb/day)	Inorganic P (lb/day)	Coliform (billions per day)
AMOCO <sup>1</sup>	1	20	2.7	1169.	182.	525	12.9	12.9	38.7	3.8
VEPCO <sup>1</sup>	1	19	3.7	37.	42.	42.	3.0	1.2	0.3	2.9
Yorktown Nat'l Park <sup>2</sup>	1	17	0.1	108.	3	3	3	3	3	3
Naval Weapons <sub>2</sub> Station	1	14	0.6	132.	3	3	3	3	3	3
Camp Peary <sup>2</sup>	1	13	0.1	18.	3	3	3	3	3	3
Town of Toano <sup>2</sup>	1	5	<0.1	17.	3	3	3	3	3	3

<sup>1</sup> Data supplied by Betz Environmental Engineers.

<sup>2</sup> Data from Hyer, et al., 1975.

<sup>3</sup> Nutrient and bacterial data not available.

there having been two different field surveys with a two-week break between. The original schedule for field sampling called for the second portion of the survey to be conducted immediately after the first half. However, 1.4" of rainfall were recorded at West Point on June 17, 1976. There was additional rain for several days, followed by a several day dry period and then 1.5" of rain on June 26. No additional rainfall was recorded between June 26 and the second portion of the field survey.

For estuaries the size of the York, it normally is not possible to survey the entire area intensively at one time, so field surveys are done in stages. The lengthy gap between surveys and the heavy rainfall occurring in that period make this data set less desirable than the one that would have resulted if there had been no rain. However, the estimates of nonpoint loadings provided by Malcolm Pirnie Engineers allow for the model to be calibrated in spite of the rainfall and runoff.

Verification data consisted of a slack water run made on September 13, 1976. Samples were taken at high water slack as it progressed upstream. The samples were taken between 10:00 a.m. and 2:00 p.m. and so the model prediction was made at high noon, model time. Results are shown in Figures 16 to 24. Fecal coliform is not included since the data are inadequate for comparison.

#### B. Model Sensitivity

One way of judging whether a model is reliable is to see if it can reproduce a known set of conditions (verification).

York River Salinity Verification-LWS September 13, 1976

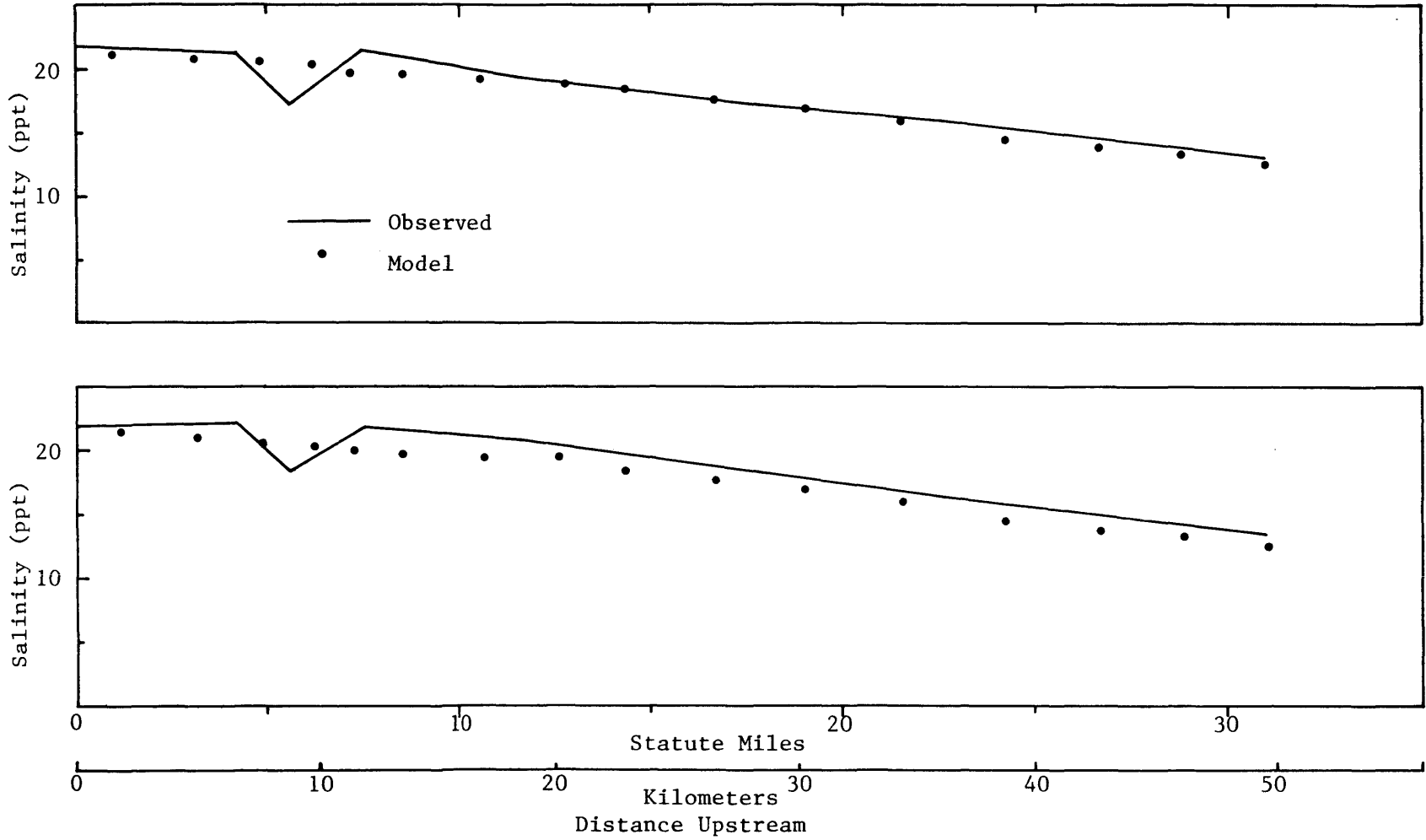


Figure 16. Verification model predictions and observed salinity values.

York River Organic Nitrogen - LWS Sept. 13, 1976

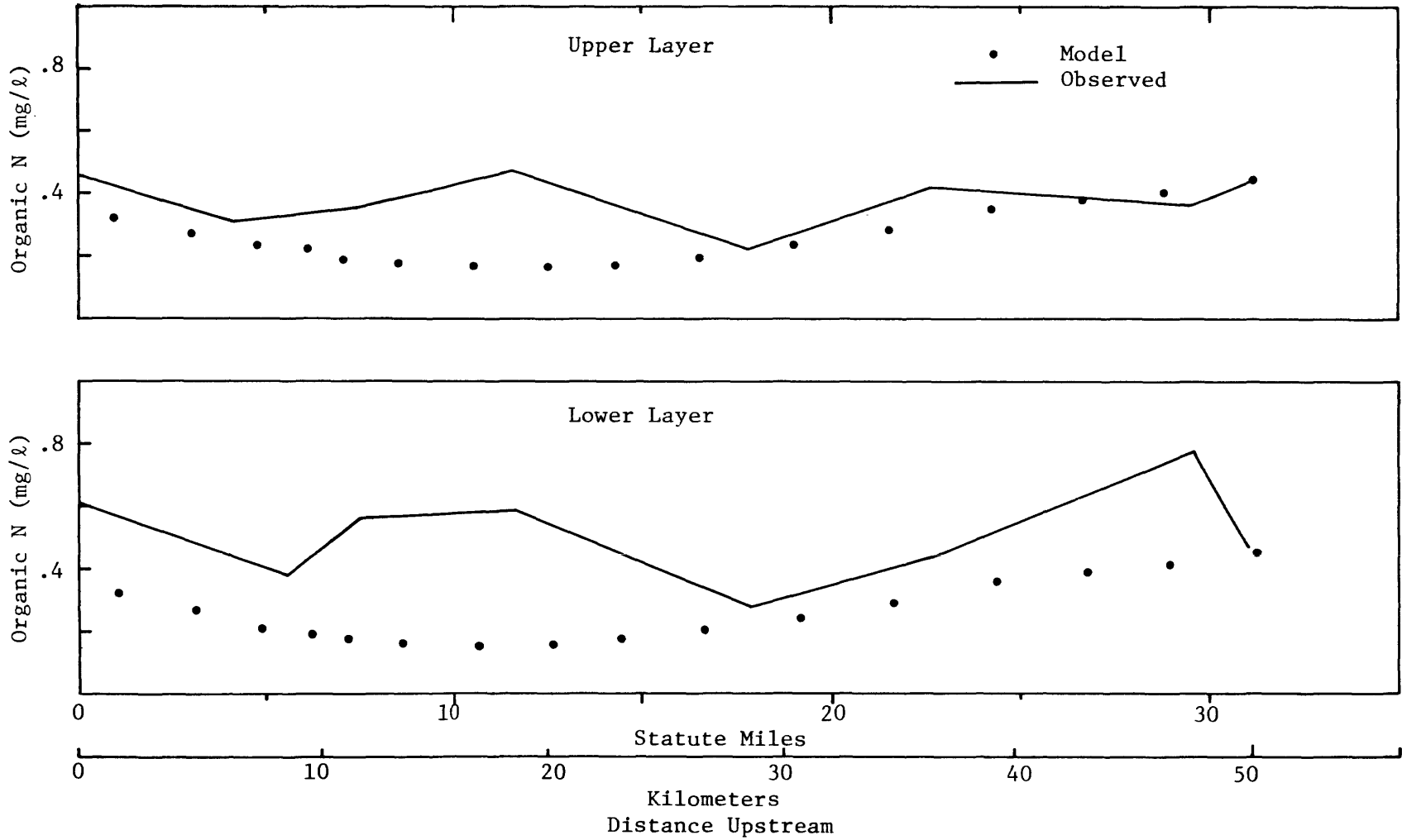


Figure 17. Verification model predictions and observed organic N values.

York River Ammonia Nitrogen - LWS Sept. 13, 1976

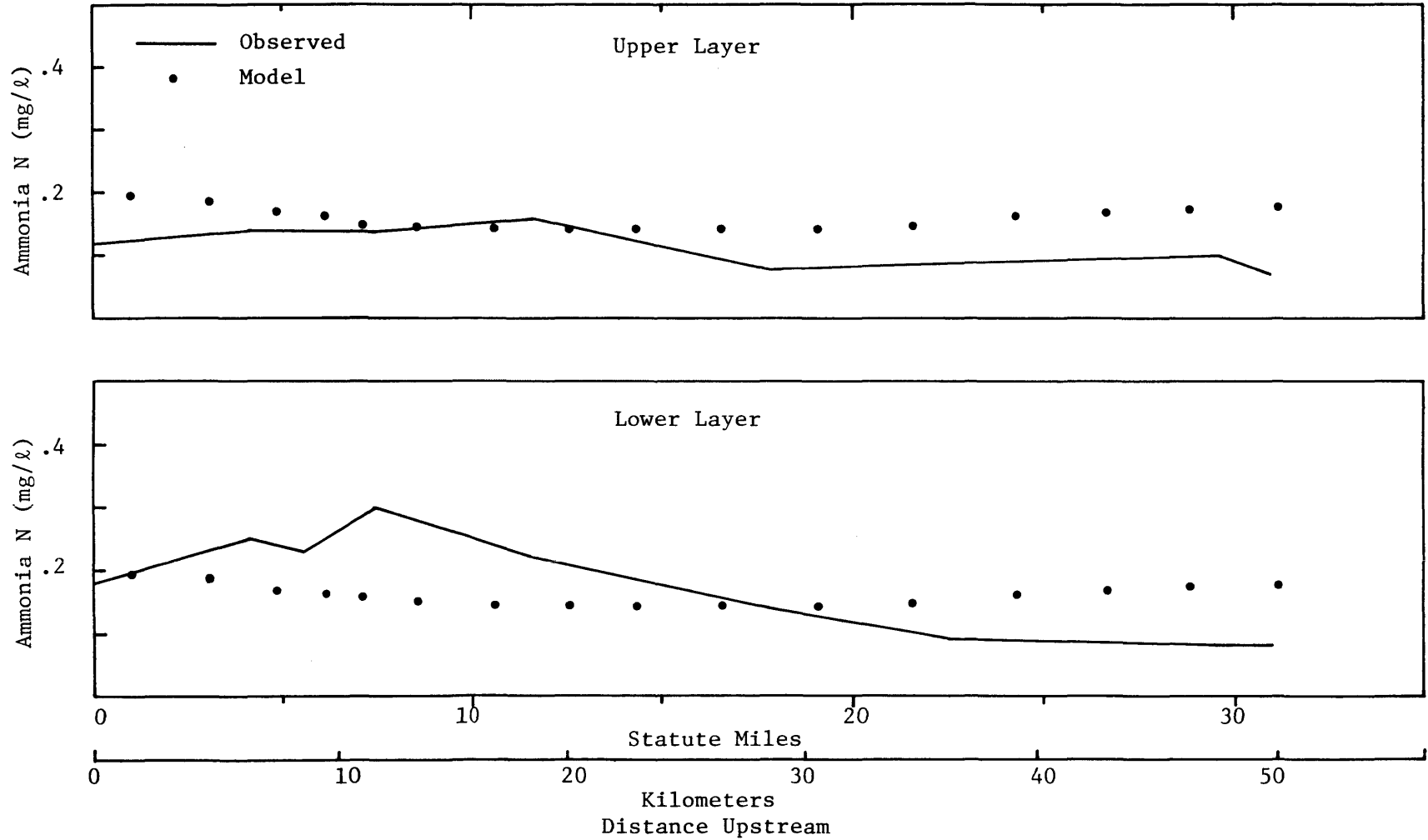


Figure 18. Verification model predictions and observed ammonia N values.

York River Nitrate plus Nitrite - LWS Sept. 13, 1976

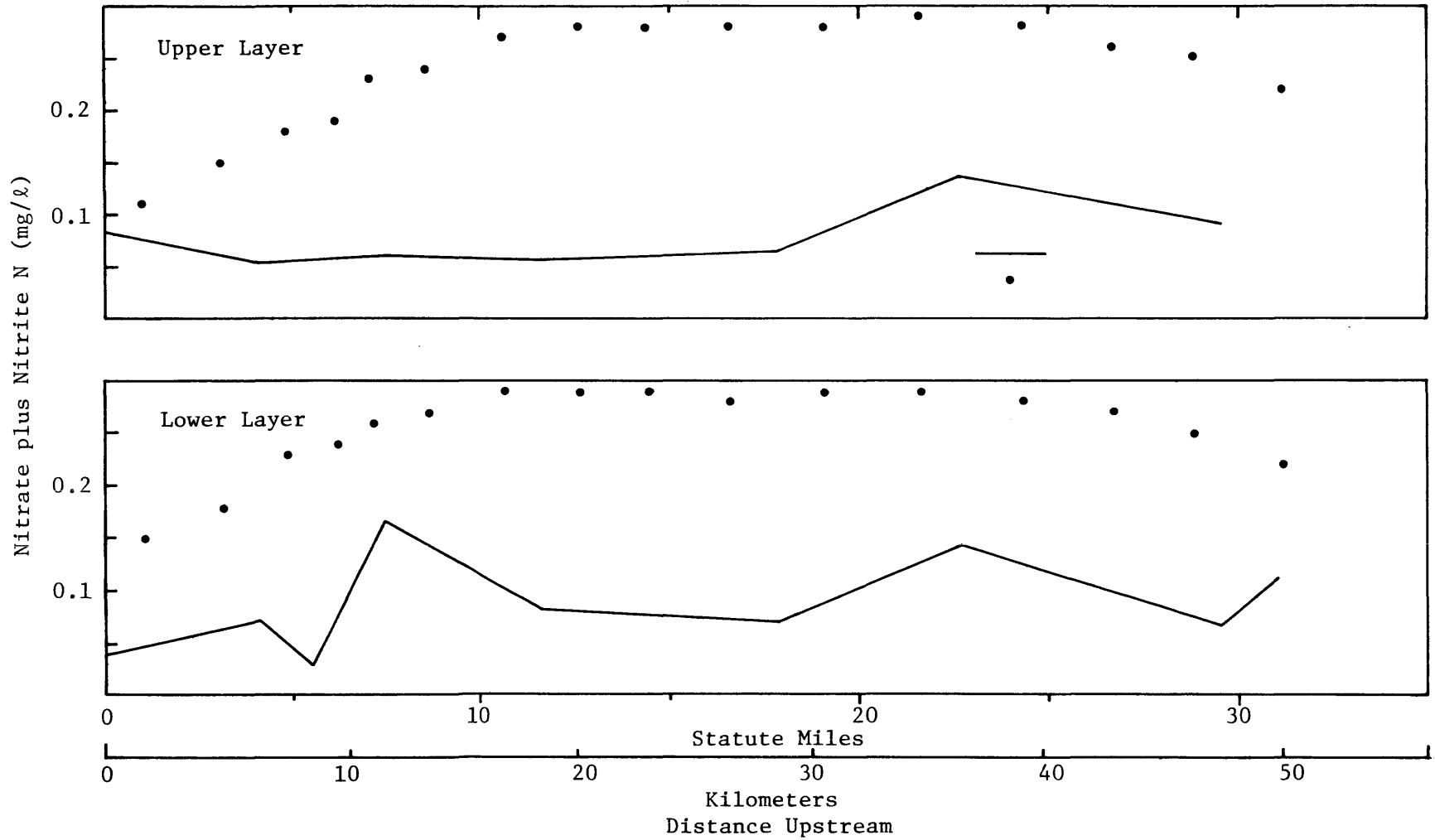


Figure 19. Verification model predictions and observed nitrate plus nitrite N values.

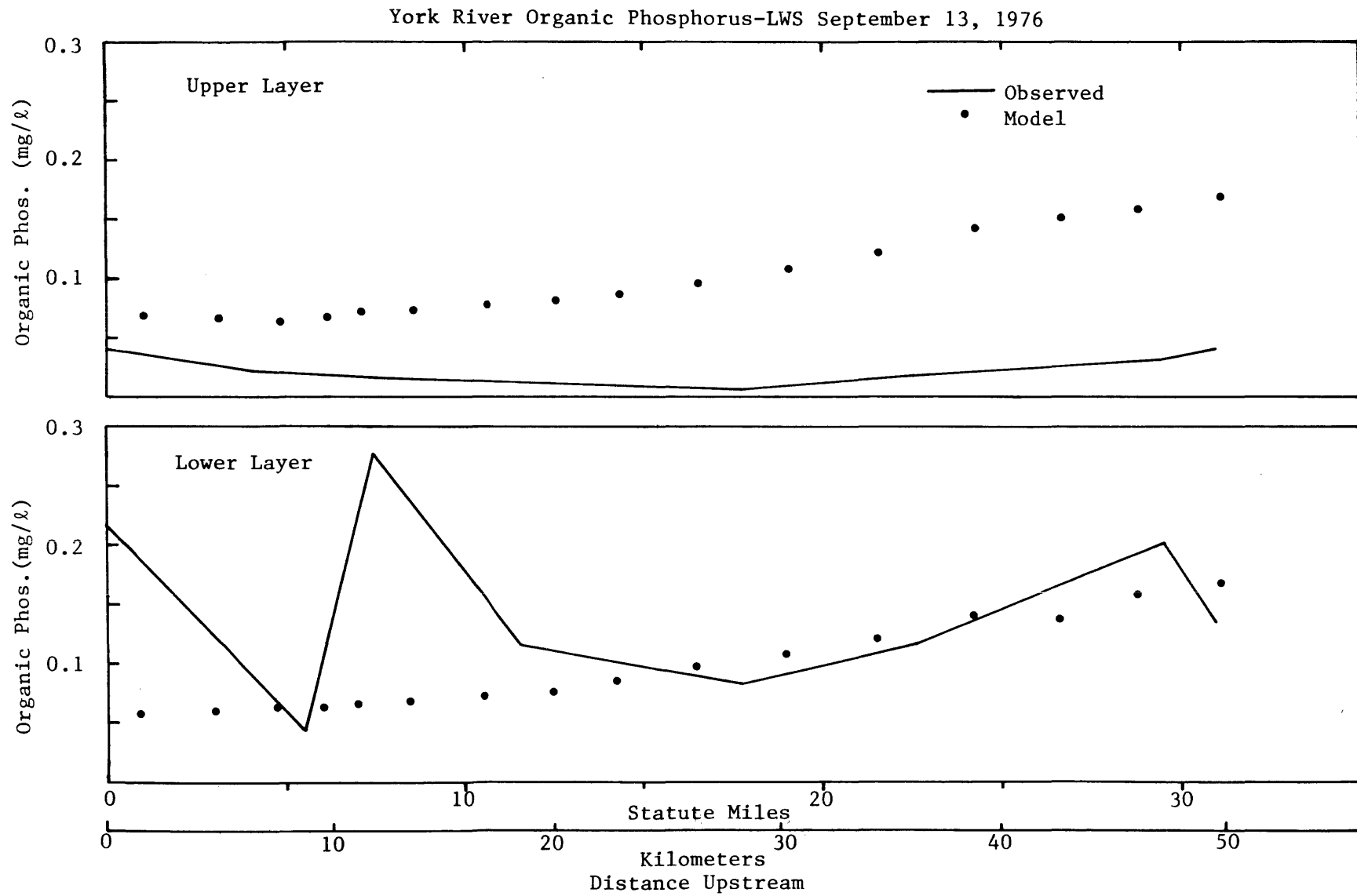


Figure 20. Verification model predictions and observed organic phosphorus values.

York River Inorganic Phosphorus-LWS September 13, 1976

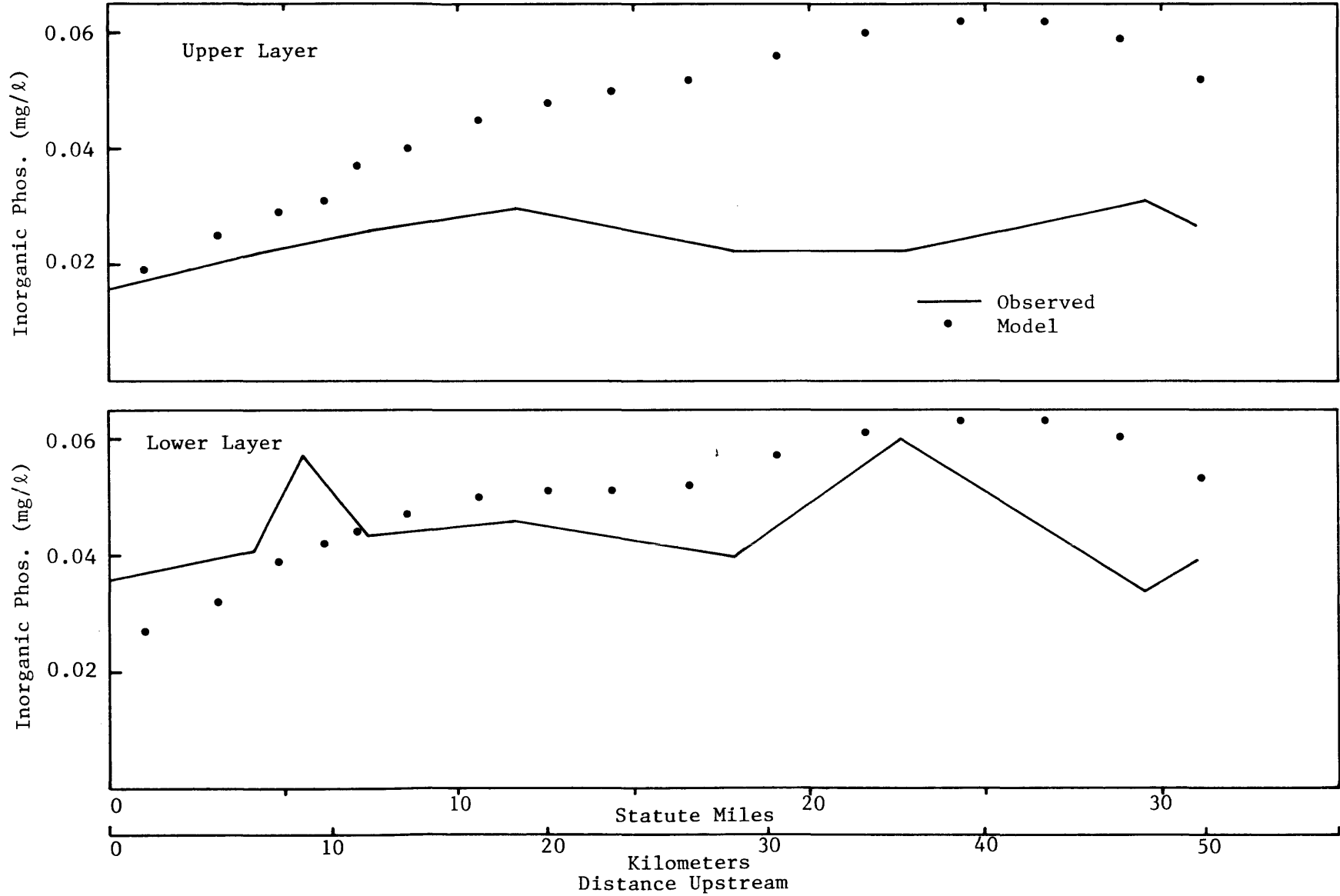


Figure 21. Verification model predictions and observed inorganic phosphorus values.

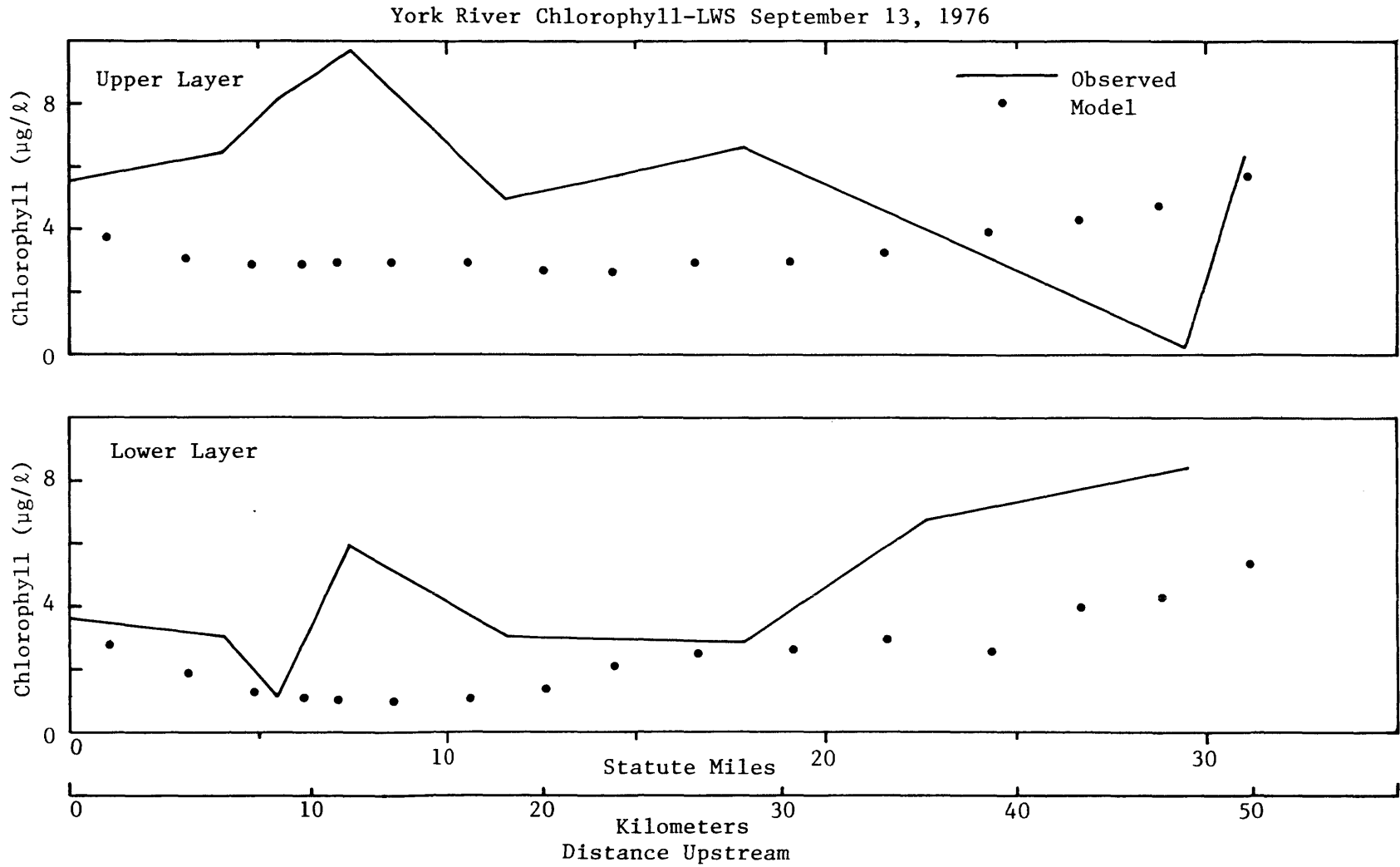


Figure 22. Verification model predictions and observed chlorophyll values.

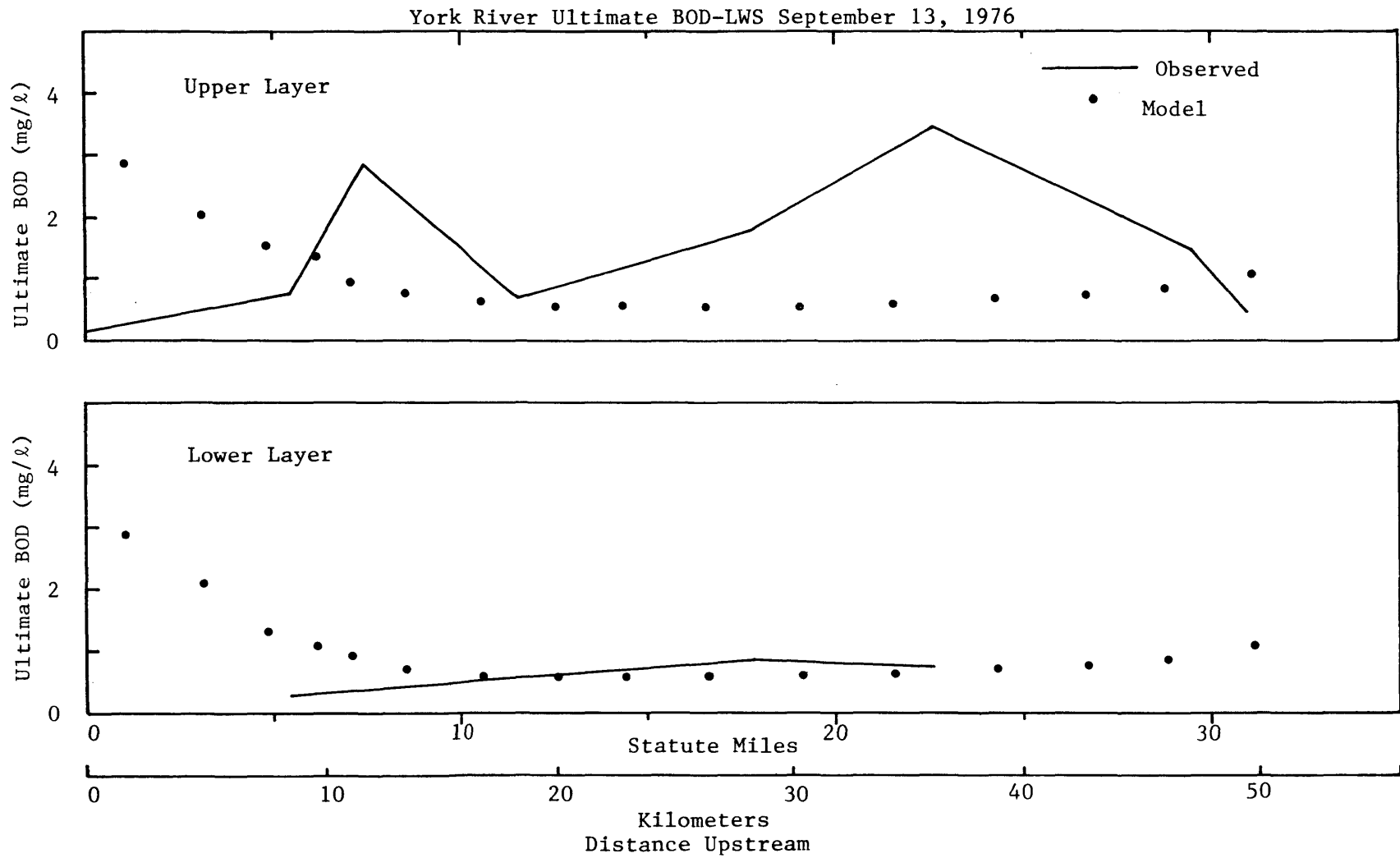


Figure 23. Verification model predictions and observed UBOD values.

York River Dissolved Oxygen- LWS September 13, 1976

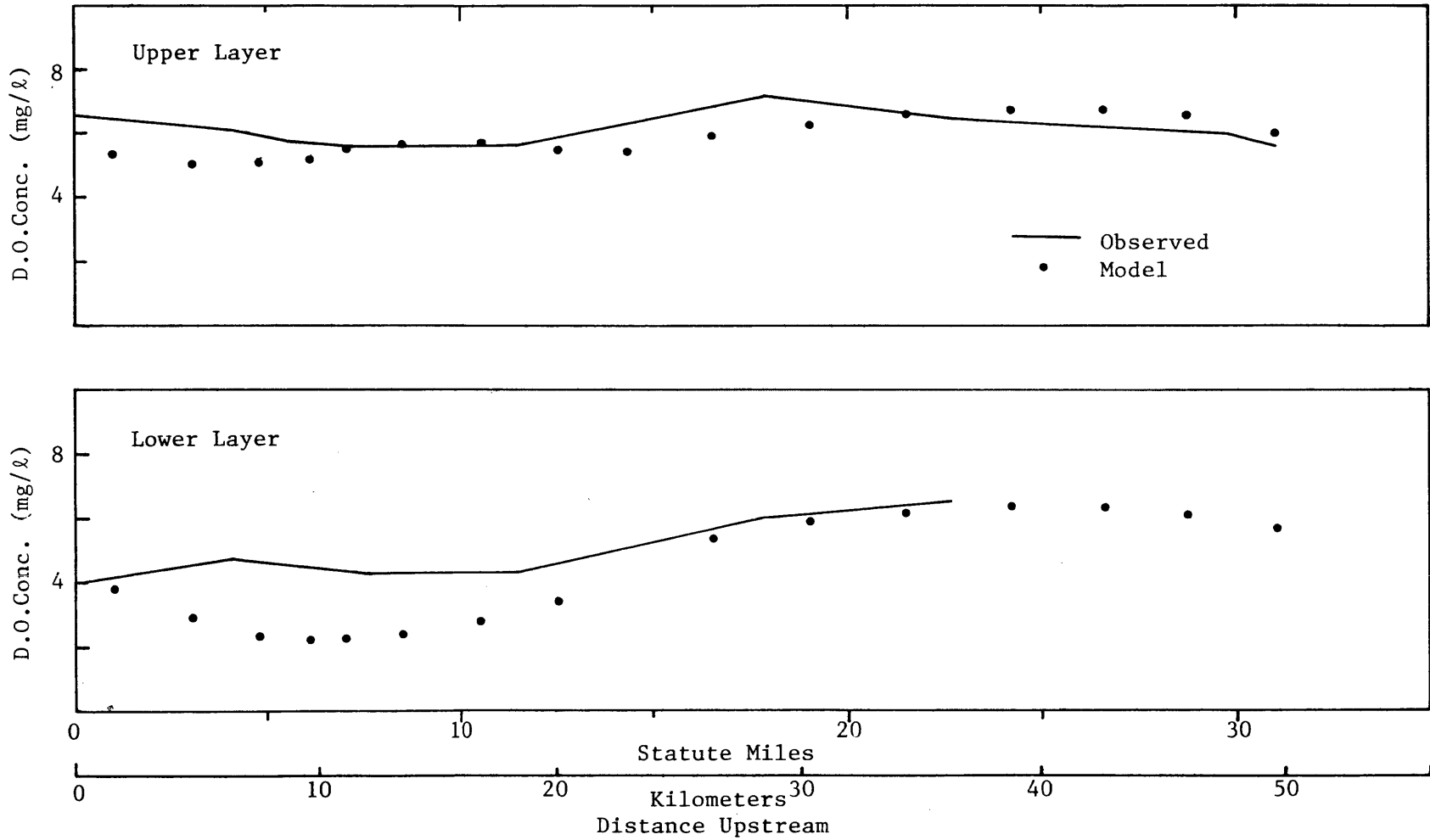


Figure 24. Verification model predictions and observed DO values.

Another check of a model is to see if variations in input cause any difference in output. This quality of a model is called sensitivity. A model which gives essentially the same result no matter what the input is clearly of little use in projections, unless there is good reason to believe that the real estuary ("prototype") is just as insensitive as the model indicates. The model inputs of most concern are:

- point source loadings (since this is chiefly what projections are about);
- dispersion coefficient and the constants associated with two-layer circulation, in order to clarify the role of these numbers;
- fresh-water inflow and boundary conditions, since these are perforce changed between calibration and verification, so that there is a need to see just how important they are;
- certain decay constants, such as those for BOD and coliform bacteria.

Sensitivity tests were made to show the response of the model to the foregoing changes in inputs.

Figure 25 shows the carbonaceous BOD distributions that result when the point sources were either doubled or eliminated. There is little difference between the curves. This insensitivity is due to the great volume of the York River; a single reach can contain as much as  $3.5 \times 10^9$  ft<sup>3</sup>. If one were to put a contaminant into this volume at a rate of  $10^4$  lb/day, it would take about three weeks to reach a level of one ppm, even ignoring decay and flushing.

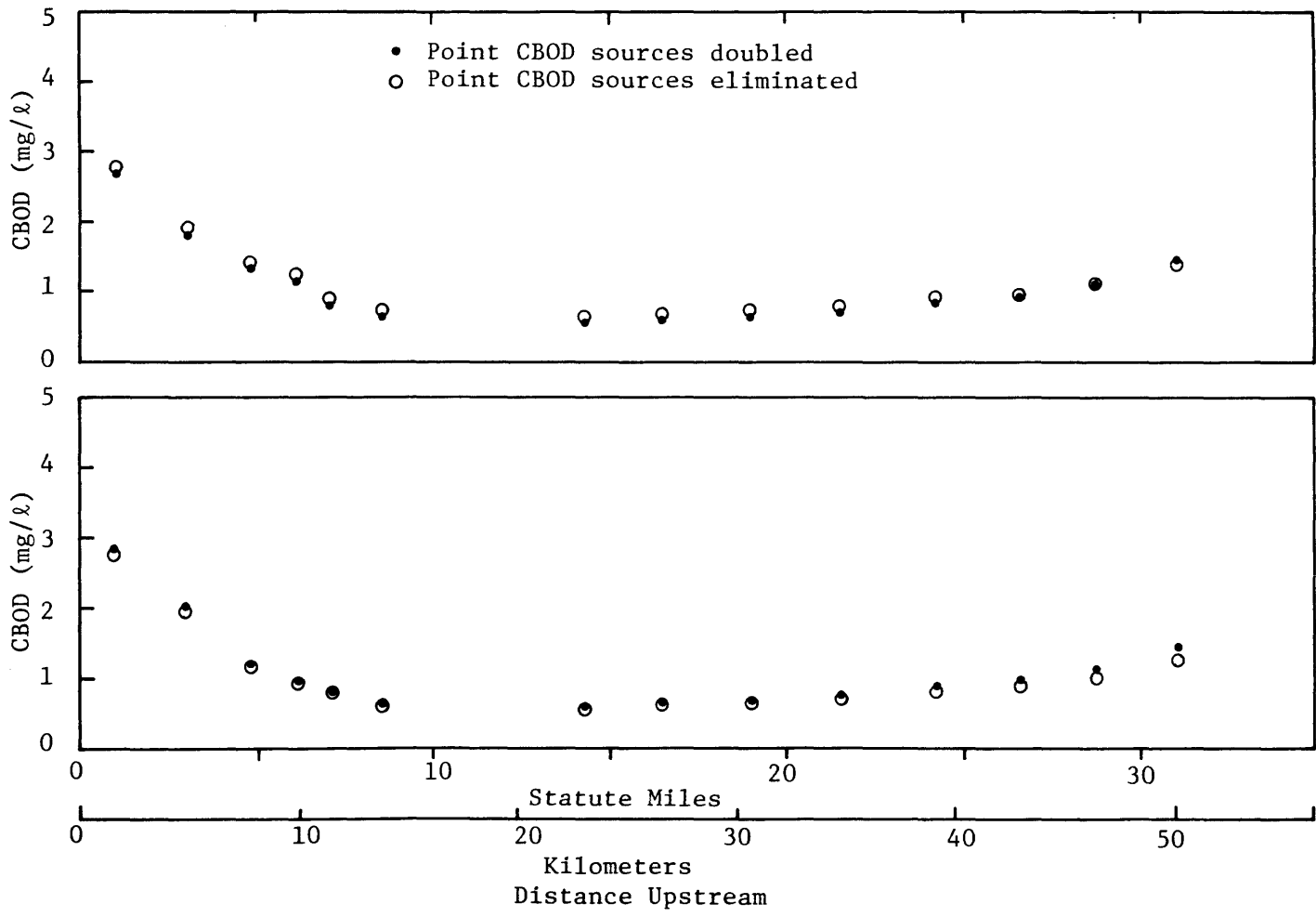


Figure 25. Model predictions for CBOD with point source loads altered.

Figure 26 shows the effect of variations in dispersion coefficient on the salinity distribution. The formula for dispersion coefficient has only one adjustable factor,  $\beta$ . Calibration was achieved with  $\beta = 2$ . Figure 26 shows the salinity distribution with  $\beta = 0.2$ ,  $\beta = 2$  and  $\beta = 20$ . As can be seen, the salinity results are not highly sensitive to this constant. The sensitivity of salinity to estuarine circulation parameter  $\nu R_a$  is shown in Figure 27. Decreasing this parameter below the calibration value had no appreciable effect. The sensitivity of the salinity distribution to changes in the freshwater inflow is shown in Figure 28. Again the calibration value is the central number. The sensitivity of salinity to changes in the boundary conditions downstream is shown in Figure 29.

Tests were made to determine the response of the BOD distribution to changes in the BOD decay rate. These are shown in Figure 30. The dependence is only slight, owing to the competing mechanisms for removal of BOD. The same is true for the oxidation of ammonia, as shown in Figures 31 and 32. The response of fecal coliform distribution to variations in dieoff rate is shown in Figure 33.

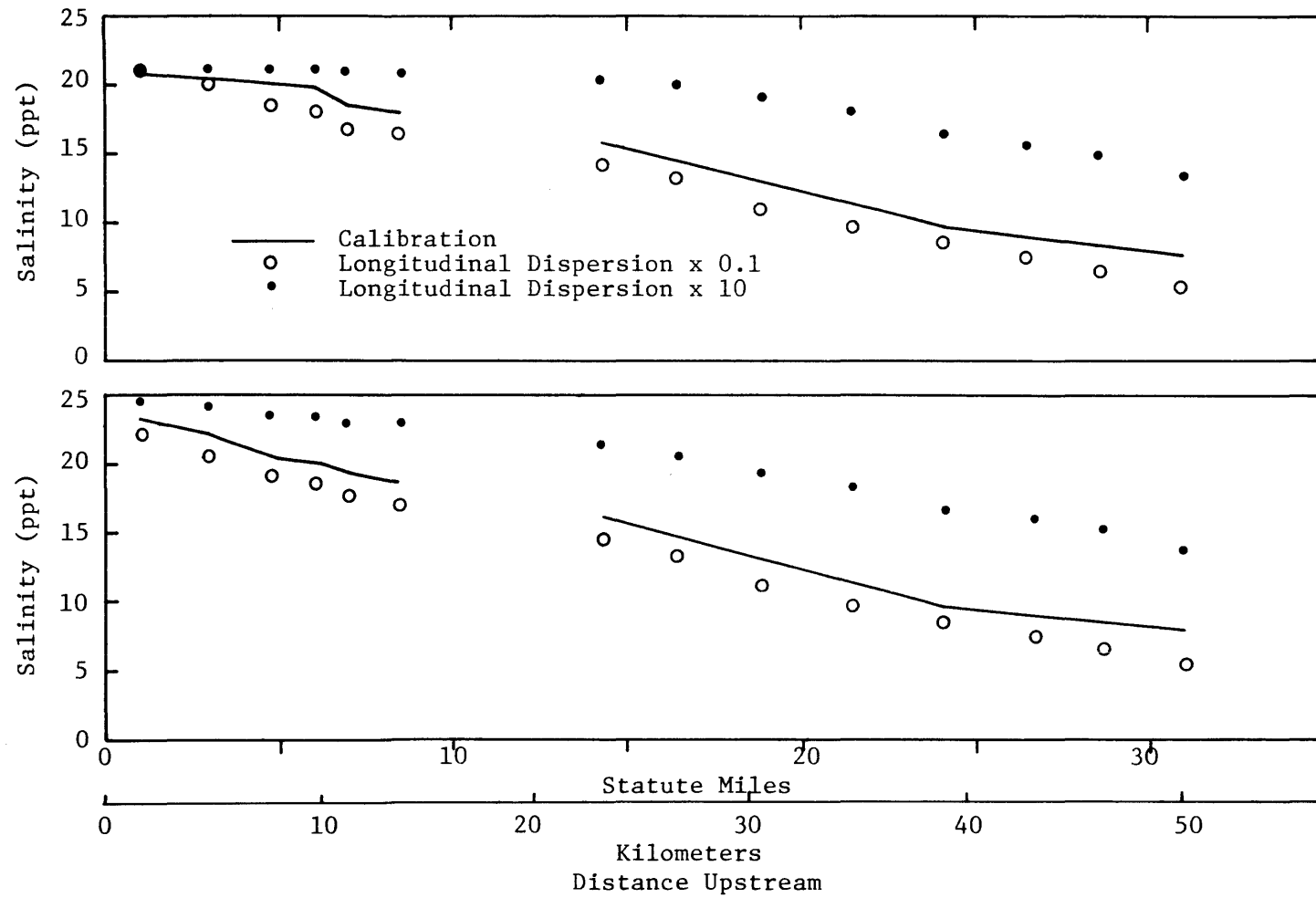


Figure 26. Sensitivity of model predictions of salinity to variations in dispersion coefficient.

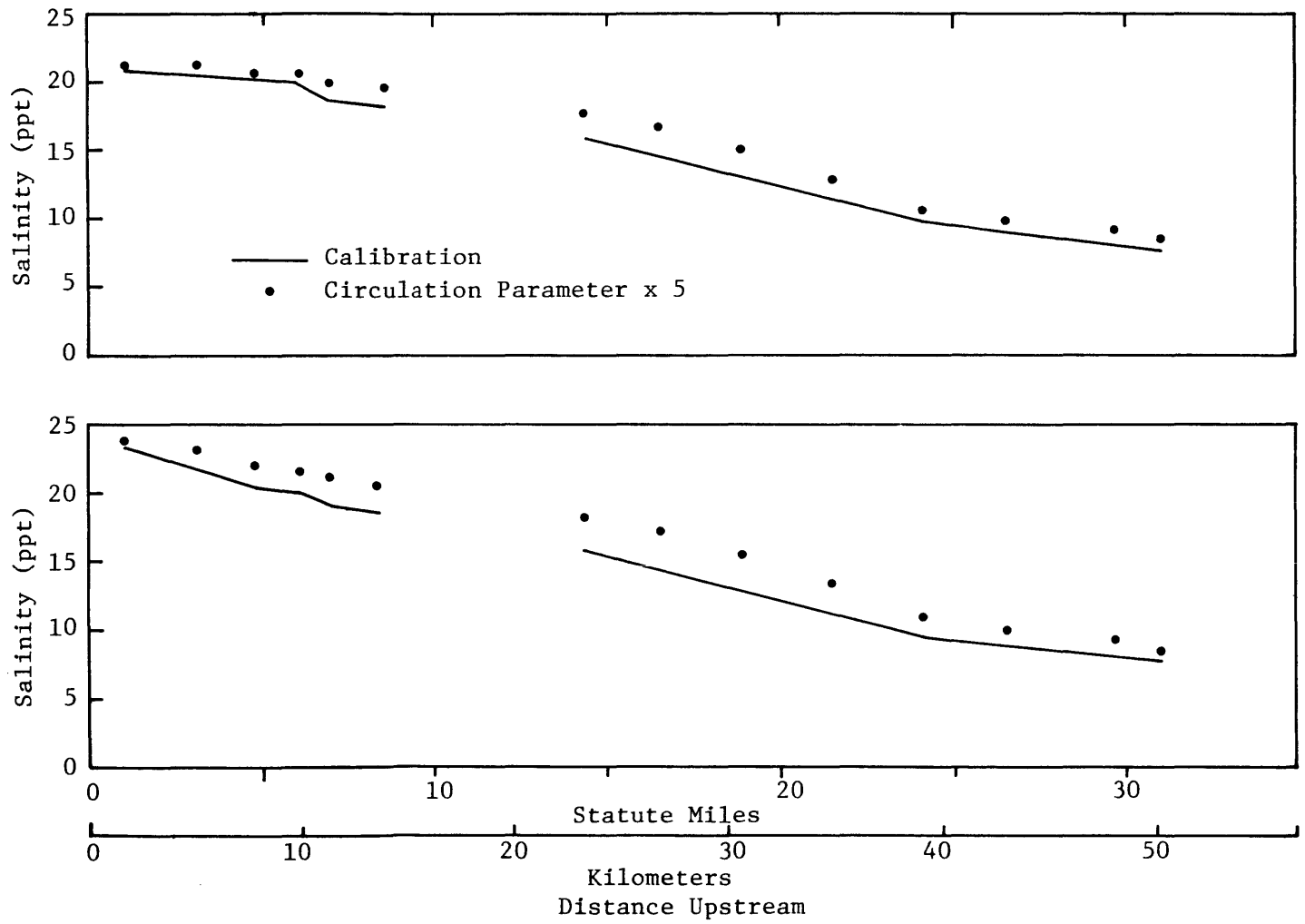


Figure 27. Sensitivity of model predictions of salinity to variations in the circulation parameter ( $\nu Ra$ ).

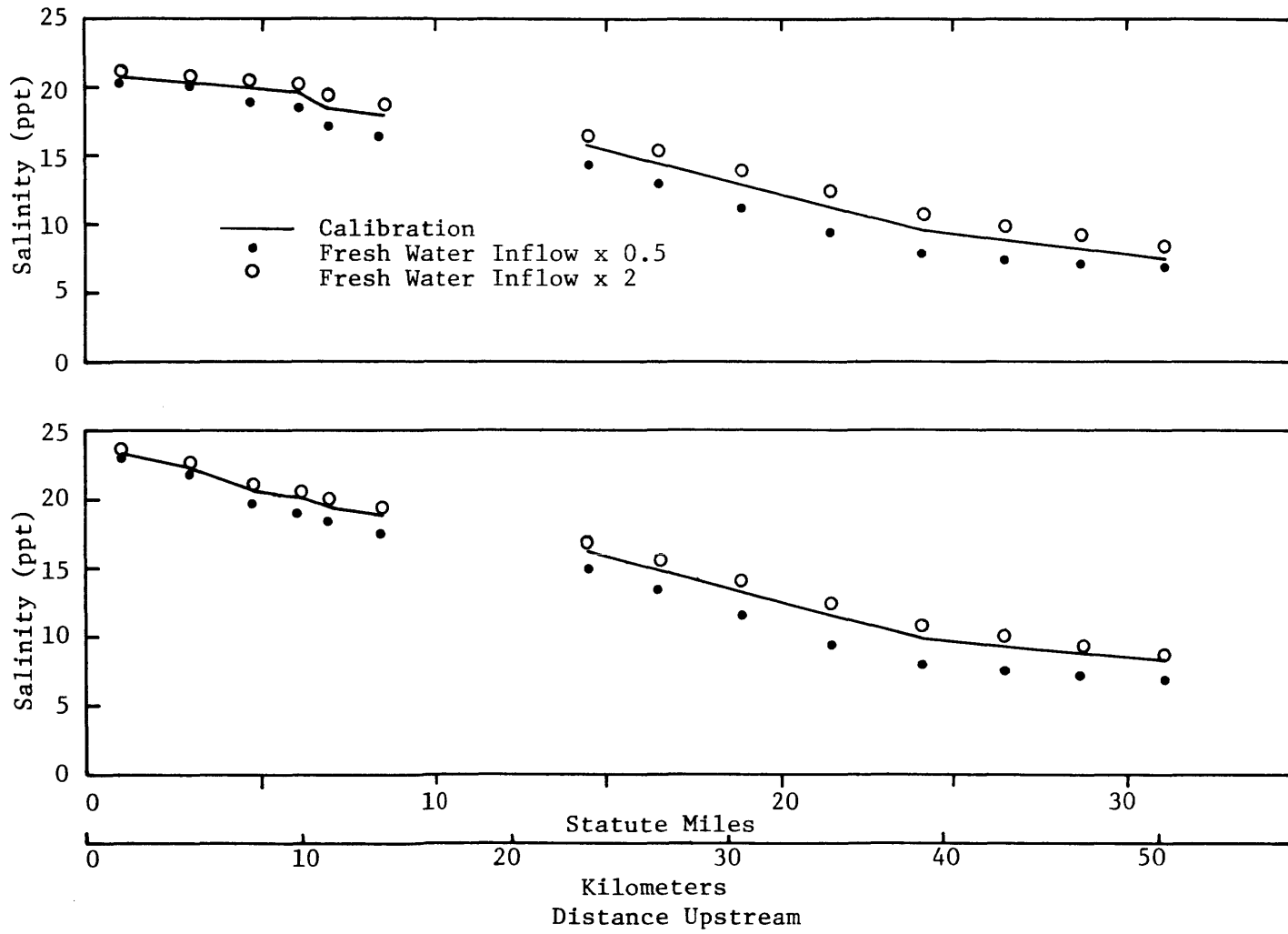


Figure 28. Sensitivity of model predictions of salinity to variations in freshwater inflow.

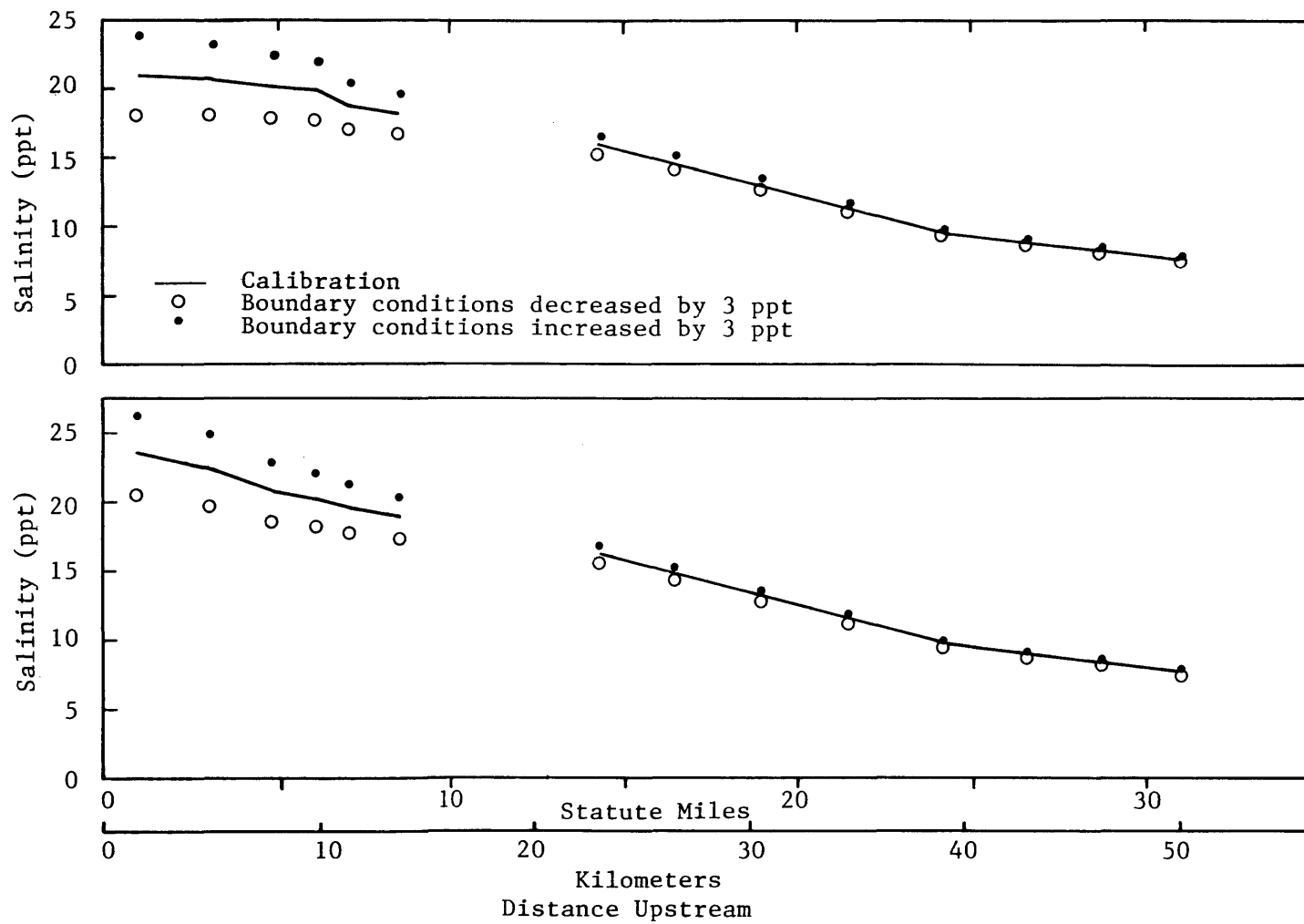


Figure 29. Sensitivity of model prediction for salinity to downstream boundary conditions.

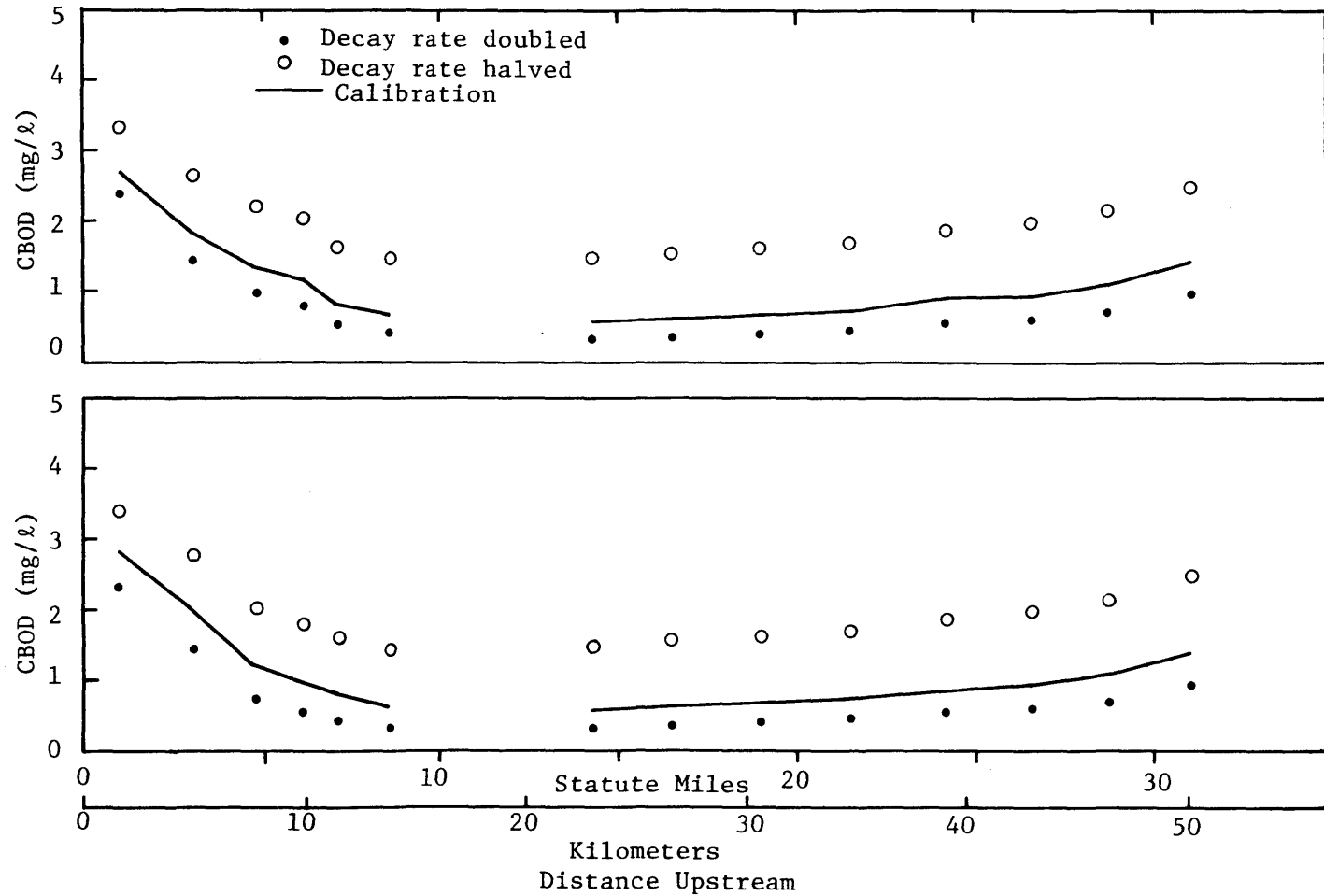


Figure 30. Sensitivity of CBOD prediction to altered decay rate.

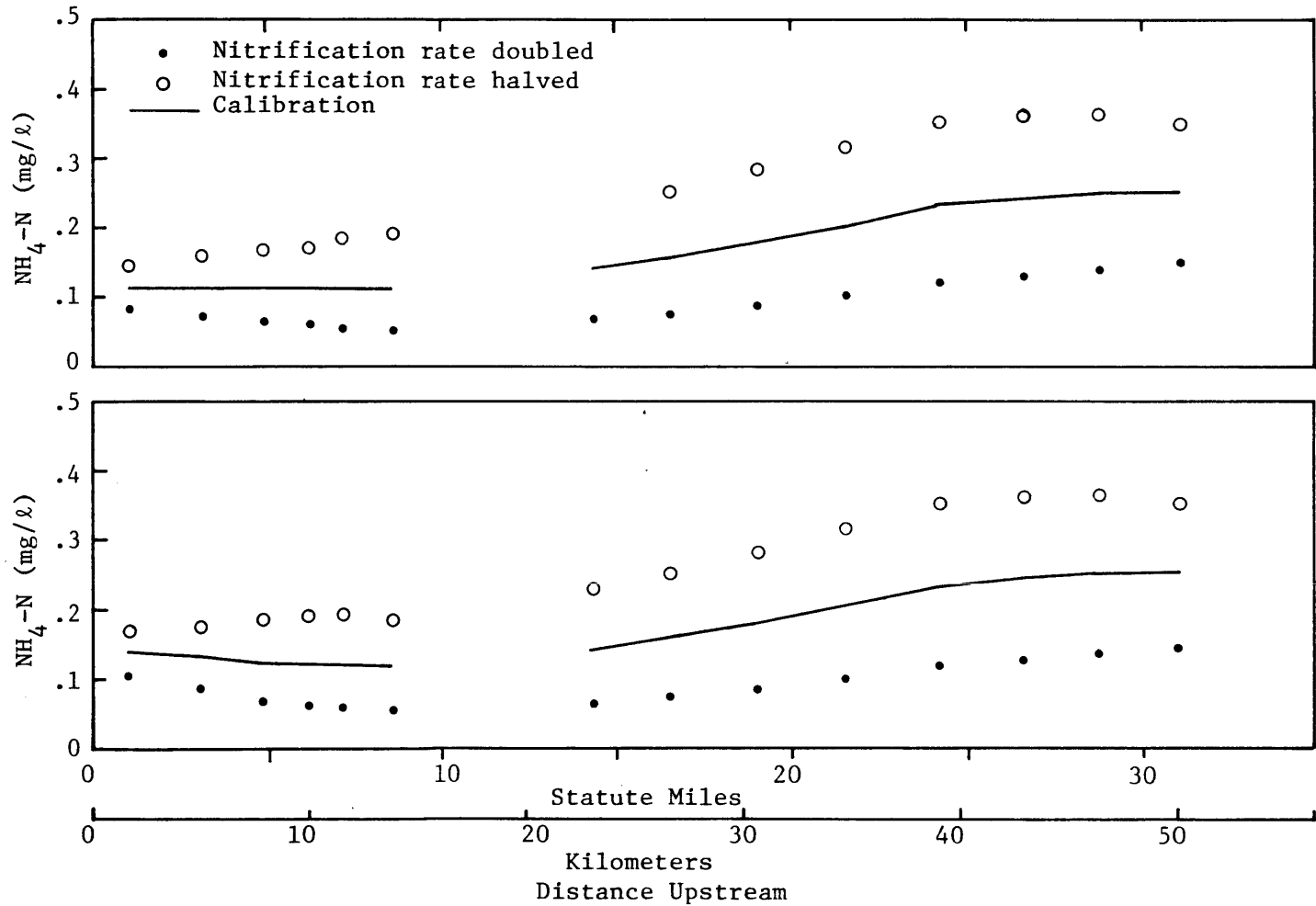


Figure 31. Sensitivity of model predictions of ammonia-nitrogen to changes in nitrification rate.

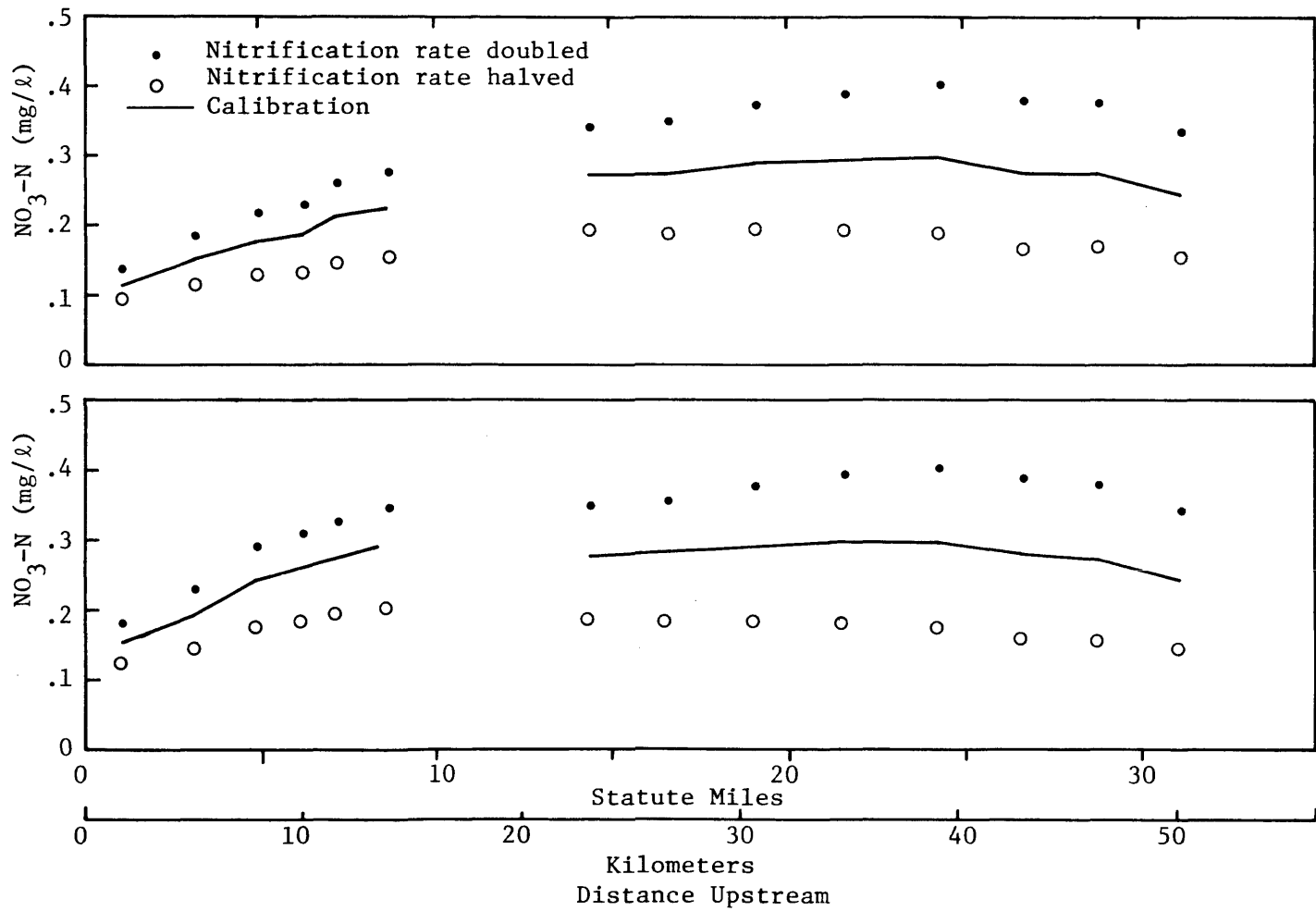


Figure 32. Sensitivity of model predictions of nitrate-nitrogen to changes in nitrification rate.

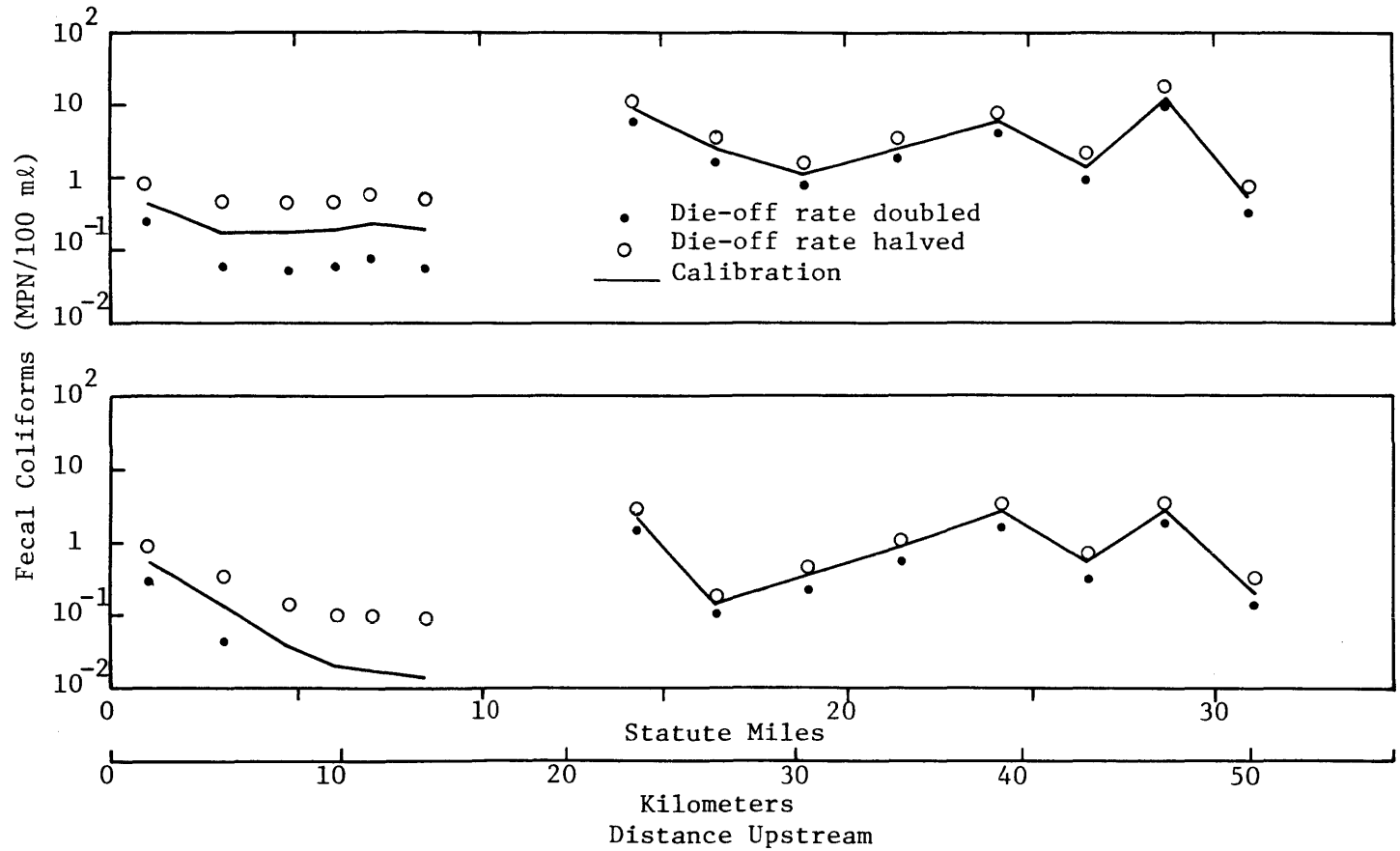


Figure 33. Sensitivity of fecal coliform predictions to altered die-off rate.

### C. Discussion

Water quality in the York River generally was quite good, with the exception of dissolved oxygen in the deep waters opposite Yorktown. In the upper layers, the daily average DO stayed above 5 mg/l except for Transect Y-2, located about five nautical miles from the river mouth. This transect is quite close to the construction at Gloucester Point where the channel is narrow (one kilometre or less) and very deep (about 30 metres). It is possible that water quality in this region is influenced by local dynamic effects not included in the model, such as upwelling or other secondary circulation.

Dissolved oxygen in the deep area between Gloucester Point and the river mouth was low (values as low as 2 mg/l were recorded) at the time of the intensive survey. This appears to be a naturally occurring phenomenon and not the result of human activities. It appears that the sill (depth around 10 metres) at the mouth of the river restricts tidal exchange and thus reduces the supply of oxygen received from Chesapeake Bay during flood tide. This relatively stagnant pool of water persists unless or until overturning takes place. Jordan's data (1975) show this condition alternately appearing and disappearing during the summer months, possibly in response to meteorological events such as extreme high tides or strong winds. The correlation between dissolved oxygen stratification and salinity stratification is not strong, suggesting that oxygen levels, once replenished, subside gradually.

The model calibration for dissolved oxygen shows very good fit but the agreement was less good for the verification run. During the slack water survey of September 13, 1976, the observed DO never went below 4 mg/l even in the deeper layer, but the model predicted DO levels below 3 mg/l. This difference probably is due to some change in the dynamics of the estuary which was not included in the mode. Nonetheless, the model can be considered to give reasonable, if conservative, results and to be useful for waste load allocation studies.

Observed chlorophyll "a" levels are below ten micrograms per litre and far below bloom conditions. As with dissolved oxygen, the agreement between field observations and predictions was better for the calibration than for the verification. One likely reason for this is that the same turbidity levels were used for both runs. No turbidity measurements were made during the slack survey, it was not considered justifiable to alter the value used in the model. Lower turbidity would have improved the fit between field observations and verification predictions. Biologists also contend that the phytoplankton population will be changed in composition and identity between the beginning of July and the middle of September. Therefore, it is believed that more importance should be given to reproducing the June-July case, since these are closer to the maximum stress conditions.

Conditions observed for nutrients are consistent with those observed for chlorophyll, namely that nutrients generally are too low to support an algal bloom even if the constraint of light limitation were removed. The verification predictions show nitrite plus nitrate-nitrogen and inorganic phosphorus concentrations at higher levels than those observed in the river. This is concomittant with the low chlorophyll levels predicted and the same remarks apply. Additionally, it should be noted that the inorganic phosphorus concentrations are close to the detection limit, so that the error is small in absolute terms, even though it may appear to be large in terms of percentages.

The data base for BOD calibration was quite small, rarely exceeding six measurements for one layer at each station. In many cases, the number of measurements is three or less, and for the case of the maximum at river mile 14 (see Figure 13), only a single measurement was obtained from each layer. Thus, a large part of the disagreement between model predictions and field observations is the result of uncertainties in the data base. Aside from this "spike", the model reproduced the general level of BOD in both the calibration and verification runs.

Fecal coliform observations in the field also consist of two to six measurements per point. Observed values of fecal coliforms in many cases are less than 0.5 MPN/100 ml with individual determinations ranging as low as 0.1 MPN/100 ml. High coliform counts do not appear to be a problem in the York

River, either now or in the future, since observed counts generally were low and there is an enormous volume of water available to dilute influent wastes.

In summary, the water quality of the York River is good, with adequate oxygen levels, low concentrations of chlorophyll "a" and nutrients, and extremely low fecal coliform counts. The single problem was the occurrence of low dissolved oxygen concentrations in the deep waters lying between Gloucester Point and the river mouth. The water quality model has demonstrated its ability to reproduce the most critical aspects of water quality and to be useful for waste load allocation studies.

## V. SUMMARY AND CONCLUSIONS

1. The downstream reaches of the York River are quite deep, in places exceeding 25 meters. As a result, the lower layers are periodically depleted of oxygen.
2. The York River is more than two miles wide in many places. Two-layer estuarine circulation is a prominent feature of the York.
3. A water quality model was constructed and calibrated for the York River. This model was "quasi-three-dimensional", having two layers and three lateral divisions per segment. The model also included gravitationally induced two-layer mean flow.
4. Ten water quality components were modeled: salinity, fecal coliform, dissolved oxygen, carbonaceous BOD, chlorophyll, three species of nitrogen and two of phosphorus.
5. Field data for calibration of the model were collected during an intensive survey in June and July, 1976. Verification data were obtained in a slack water run in September, 1976.
6. The model is able to reproduce the important water quality features of the York River and is suitable for use in development of waste load allocation and similar studies.

## REFERENCES

- Carritt, D. E. and E. J. Green. 1967. "New Tables for Oxygen Saturation of Seawater." *Jo. Mar. Res.*, Vol. 25, No. 2.
- Cronin, W. B. 1971. "Volumetric, Areal and Tidal Statistics of the Chesapeake Bay Estuary and its Tributaries", CBI Special Report 20, Ref. 71-2, March.
- Di Toro, D. M., D. J. O'Connor and R. V. Thomann. 1971. "A Dynamic Model of the Phytoplankton Population in the Sacramento-San Joaquin Delta." *Adventures in Chemistry Series*, No. 106, American Chemical Society, pp. 131-180.
- Elmore, H. L. and W. F. West. 1961. "Effect of Water Temperature on Stream Reaeration." *Proc. ASCE*, 87(SA6).
- Hansen, D. V. and M. Rattray, Jr. 1965. "Gravitational Circulation in Straits and Estuaries." *Jo. Mar. Res.* 23(2).
- Hansen, D. V. and M. Rattray, Jr. 1966. "New Dimensions in Estuary Classification." *Limnology and Oceanography*, Vol. XI(3).
- Holley, E. R., D. R. F. Harleman and H. B. Fischer. 1970. "Dispersion in Homogeneous Estuary Flow." *Jo. ASCE*, Vol. 96, No. HY8, pp. 1691-1709, August.
- Hyer, P. V., A. Y. Kuo, C. S. Fang and W. J. Hargis, Jr. 1975. "Hydrography and Hydrodynamics of Virginia Estuaries, VIII. Mathematical Model Studies of Water Quality of the York River System." *VIMS Special Report No. 104 in Applied Marine Science and Ocean Engineering*, October.
- Hyer, P. V., A. Y. Kuo and B. J. Neilson. 1977. "Water Quality Models of Back and Poquoson Rivers, Virginia." *VIMS SRAMSOE No. 144*, June.
- Hyer, P. V. and J. Jacobson, 1976. "Hydrography and Hydrodynamics of Virginia Estuaries, IX. Mathematical Water Quality Study of Great Wicomico River and Cockrell Creek", *Virginia Institute of Marine Science, Special Report No. 120 in Applied Marine Science and Ocean Engineering*, Gloucester Point, Virginia 23062, September.
- Jordan, R. A., et al., 1975. "Yorktown Power Station Ecological Studies, Phase II: Final Technical Report." *VIMS Special Scientific Report No. 76*, May.

## References (cont'd)

- O'Connor, D. J. and W. E. Dobbins. 1956. "Mechanics of Reaeration in Natural Streams." Proc. ASCE, 82(SA2).
- Seitz, R. C. 1971. "Drainage Area Statistics for the Chesapeake Bay Freshwater Drainage Basin." CBI Special Report 19, Ref. 71-1, February.
- Thomann, R. V., D. M. Di Toro and D. J. O'Connor. 1974. "Preliminary Model of Potomac Estuary Phytoplankton." J. ASCE, Vol. 100, No. EE3, pp. 699-715, June.
- U. S. Geological Survey, Water Resources Division. "Water Resources Data for Virginia, Water Year 1976." U. S. Geological Survey Water Data Report VA-75-1, Report No. USGS/WRD/HD/-76/035, September, 1976.

APPENDIX A

Input Constants

## Independent Variables Used as Input to Model

<u>Input</u>	<u>Source</u>
River Channel Geometry	Vims Bathymetry Survey
Drainage Basin Area	Va. Div. of Water Resources Bulletin
Tidal Current Amplitude	Current meter measurements simultaneous w/intensive survey
Fresh Water Inflow	U. S. G. S. flow gauges
Incident Solar Radiation	Concurrent Pyroheliometer Data taken by Langley Research Center
Bottom Oxygen Demand	VIMS Surveys, 25 June and 2 July, 1976
CBOD Decay Rate	VIMS Intensive Survey, June and July, 1976

Values of Rate Constants and Coefficients used  
in York River Water Quality Model

<u>Constant (Symbol)</u>	<u>Units</u>	<u>Value used in Model</u>
Saturation Light Intensity (RIS)	$\frac{\text{langley}}{\text{day}}$	200
Saturation Phytoplankton Growth Rate (GSAT)	$\text{day}^{-1}$	2.75
Phosphorus Michaelis Constant (KMP)	$\frac{\text{mg P}}{\text{l}}$	.005
Nitrogen Michaelis Constant (KMN)	$\frac{\text{mg N}}{\text{l}}$	.05
Plankton Settling Rate (KCS)	$\text{day}^{-1}$	0.
Endogenous Respiration Rate (RRESP)	$\frac{\text{day}^{-1}}{\text{°C}^{-1}}$	.004
Carbon Chlorophyll Ratio (AC)	$\frac{\text{mg}}{\mu\text{g}}$	.097
Nitrogen-Chlorophyll Ratio (AN)	$\frac{\text{mg}}{\mu\text{g}}$	.0136
Phosphorus-Chloro- phyll Ratio (AP)	$\frac{\text{mg}}{\mu\text{g}}$	.0029
Organic N-Ammonia Hydrolysis Rate Constant (KN12)	$\frac{\text{day}^{-1}}{\text{°C}^{-1}}$	.0025
Ammonia Nitrification Rate (KN23)	$\frac{\text{day}^{-1}}{\text{°C}^{-1}}$	.0030
Organic Phosphorus to Inorganic Phosphorus Rate Constant (KP12)	$\frac{\text{day}^{-1}}{\text{°C}^{-1}}$	.0010

<u>Constant (Symbol)</u>	<u>Units</u>	<u>Value used in Model</u>
Grazing Constant (KGRAZ)	day <sup>-1</sup>	0.12
Photosynthetic Quotient (PQ)		1.3